Helsinki University of Technology Doctoral Theses in Materials and Earth Sciences
Laboratory of Physical Metallurgy and Materials Science
Espoo 2004 TKK-ME-DT-2

NOVEL Ni-Mn-Ga ALLOYS AND THEIR MAGNETIC SHAPE MEMORY BEHAVIOUR

Outi Söderberg

Dissertation for the degree of Doctor of Science in Technology to be presented with due permission of the Department of Materials Science and Rock Engineering for public examination and debate in Auditorium V1 at Helsinki University of Technology (Espoo, Finland) on the 10th of December, 2004, at 12 o'clock noon.

Helsinki University of Technology
Department of Materials Science and Rock Engineering
Laboratory of Physical Metallurgy and Materials Science

Helsinki University of Technology
Laboratory of Physical Metallurgy and Materials Science
P.O. Box 6200
FI-02015 TKK

Available in pdf-format at http://lib.hut.fi/Diss/

Cover:
Morphological structures of the alloys $Ni_{53.5}Mn_{24.5}Ga_{22}$ and $Ni_{55}Mn_{21}Ga_{24}$. The third structure is of thermo-mechanically treated single crystalline sample of the latter alloy.

ISBN 951-22-7415-9
ISBN 951-22-7416-7 (electronic)
ISSN 1795-0074

Picaset Oy
Helsinki 2004

ABSTRACT

The ternary Ni-Mn-Ga system has already been studied for several decades. Although the present work concentrates on the alloys with the 7-layered near-orthorhombic martensite structure (**7M**) and the non-modulated tetragonal martensite structure (**T**), it introduces 37 alloys altogether, including materials that have the 5-layered tetragonal martensite (**5M**) at ambient temperature. The dissertation shows briefly how the different compositions of ternary Ni-Mn-Ga alloys affect the phase transformations and the crystallographic structures of various phases. This thesis presents new alloys with the **7M** structure and, for the first time, the Curie point of such a martensitic structure (T_{C7M}). This T_{C7M} is mainly detected in the cooling of the alloys, showing the co-occurrence of the magnetic transition and the double-step reverse transformation where the hysteresis of the Curie point is connected to the two martensitic phases.

The service temperature region of the MSM alloy depends on the existence of the proper ferromagnetic twinned martensite. Consequently, the transformation sequence of the studied **7M** and **T** alloys is investigated in more detail. According to the magnetic and crystalline transformation, the alloys are divided into six groups: ***A* (7M ambient), *B* (7M above), *C* (7M co-transition), *D* (T high), *E* (T low) and *F* (T co-transition)**. In the groups ***A, B, D*** and ***E,*** the magnetic and crystalline transitions are separated, while in the groups ***C*** and ***F*** they co-occur.

The pre-straining processes for obtaining the single-variant state in the **7M** and the **T** martensite are presented. In the compression of the **7M** alloys, three deformations to two crystallographic directions are needed, while the **T** alloys require three deformations to three crystallographic directions. However, it is also shown that with the tensile/compressive cycling of the **T** phase the full single-variant state has been obtained already, during the second cycle. The twinning stresses (σ_{tw}) needed for the martensite variant reorientation could be lowered by pre-straining close to 1 MPa in the **7M** phase, while in the **T** phase only the level 6 MPa was reached, even at elevated temperatures. The magneto-mechanical tests confirmed that the magnetically induced stress ($\Delta\sigma_{mag}$) in the **7M** structure is 1.5 MPa and in the **T** structure approximately 1 MPa. By applying the criteria of $\Delta\sigma_{mag} \geq \sigma_{tw}$ for the magnetic shape memory effect (MSME), it is obvious that MSME is possible in the **7M** structure, but it can not be obtained in the **T** structure.

Keywords:
Ni-Mn-Ga alloys, martensite, intermartensitic transformation,
twinning, magnetic shape memory

FOREWORD

It has been a part of the collaborative MSM-project, the Magnetic Shape Memory Materials –project, in which I was a member of an enthusiastic research team working in our laboratory, in the Laboratory of Biomedical Engineering and in the Laboratory of Physics. At first, I would like to thank Prof. Veikko Lindroos for his help, support and belief in my work and its success. I thank Prof. Juha Pietikäinen for originally guiding me into the world of martensite, not to mention the huge experience of the ICOMAT'02 conference. Dr. Kari Ullakko deserves thanks for his inspiration and the fact that he persuaded me to start with the present subject. I sincerely acknowledge Dr. Alexei Sozinov for his enormous help and his encouragement to finish the thesis in time for presentation. I thank Prof. Simo-Pekka Hannula for all his valuable comments and great help in the long process of writing. Especially, I thank Marjatta Aav M.Sc. (Econ.) for her patience with my peculiar English and for all her everyday help with my work. I am grateful for the friendship and great spirit of cooperation shown by all the other members of the HUT-MSM-team: Matti Aalto-Setälä B.Sc., Dr. Andrés Ayuela, Dr. Jussi Enkovaara, Eemeli Erola B.Sc., Yanling Ge M.Sc., Pekka Havola Lic.Tech., Dr. Oleg Heczko, Kaisa Huitu B.Sc., Ari Jääskeläinen M.Sc., Kari Koho M.Sc., Nataliya Lanska M.Sc., Dr. Alexander Likhachev, Dr. Xuwen Liu, Sanni Mustala M.Sc., Tina Sammi M.Sc., Jukka Seuranen M.Sc., Ladya Straka M.Sc., Sami Vapalahti M.Sc. and Jarkko Vimpari M.Sc. It has been a great pleasure and joy to work with them all, not only in the frame of scientific work, but socially as well. This same applies to staff members and the unforgettable students of the Laboratory of Physical Metallurgy and Materials Science. I thank all of them, and especially Mrs. Pirjo Korpiala, Arja Teramo B.A., Ulla Nyman Lic.Tech., Ilkka Penttinen Lic.Tech., Eero Haimi M.Sc., Dr. Risto Toivanen, Prof. Roman Nówak and Prof. Ari Lehto.

I am grateful to the Outokumpu Oyj Foundation for their grant that allowed the present work to be carried out during the year 2004. I thank Markku Kytö Lic.Tech., the representative of the Foundation, and Mrs. Riitta Tolonen for their help. I acknowledge also all the funding organisations as well as the steering boards of the HUT-MSM project: The National Technology Agency of Finland (Tekes), Outokumpu Research Oy, Metso Paper Oy, Nokia Research Center, ABB Corporate Research Oy, AdaptaMat Ltd., Technology Industries of Finland (formerly the Federation of Finnish Metal), Engineering and Electrotechnical Industries (MET), the Academy of Finland and Helsinki University of Technology.

The greatest factor in the success of this work was the availability of the Ni-Mn-Ga alloys. I wish to thank two manufacturers of Ni-Mn-Ga materials that we have had the opportunity to deal with. First, the great work on over 100 different alloys carried out at Outokumpu Research Centre in 1999-2002 is beyond all the wishes of a serious researcher. I would like to thank Dr. Pekka Taskinen, Tuija Suortti Lic.Tech., Heljä Peltola Lic.Tech. and Juha Järvi M.Sc. for all their knowledge and help with these very special materials. Furthermore, I thank Dr. Emmanouel Pagounis, Ilkka Aaltio M.Sc., Olavi Mattila B.Sc. and Mr. Tarmo Virén of AdaptaMat Ltd. for the large ingot materials obtained during 2000-2003.

My work would not have been possible without the co-operation of the Institute for Metal Physics in Kiev and especially the group of Prof. Valentin Gavriljuk. I would like to thank him for his help and friendship that has continued for over 15 years. The scientific work with Dr. Nadya Glavatska, Dr. Peter Yakovenko, Dr. Bela Shanina, Dr. Vitalij Blyznyuk, Ilya Glavatskiy M.Sc., George Mogylny M.Sc. and with many others has taught me so much and given numerous unforgettable moments both at HUT and in Kiev. I thank also Dr. Vaclav Novák from Institute of Physics ASCR in Prague for his work and help during the preparation of the *Publication VI.*

Finally, all the work carried out at the laboratory, in conferences, abroad, at lecture halls or at my computer would not have been possible without my family. I dedicate this work to my innovative and inspiring sons, Jan and Henrik, who have kept me in touch with the pleasures of day-to-day life and given me so much to live for. I thank Kenneth for his support and patience – the time given to the research and teaching was sometimes taken from something more important. Also, I would like to thank Anne-Maj and Olof. The greatest acknowledgement, however, belongs to my parents, Irja and Kalle: Without all the time and help and support that they have given to me and the boys during all these years, this work would never have been possible.

In warm memory of Pirkko, Lena and Ari.

Yours sincerely
Outi

To Jan and Henrik
Motto:
Hyvä minä, hyvä me, hyvä meidän joukkue – EsPa Titaanit ’93 juniorijalkapalloilijat.

LIST OF PUBLICATIONS I-VIII

The following publications form the integral main part of the present thesis:

I *N. Lanska, O. Söderberg, A. Sozinov, Y. Ge, K. Ullakko, V.K. Lindroos,* **Composition and temperature dependence of the crystal structure in Ni-Mn-Ga alloys**, Journal of Applied Physics **95** (2004) 8074-8078.

II *O. Söderberg, M. Friman, A. Sozinov, N. Lanska, Y. Ge, M. Hämäläinen and V.K. Lindroos***, Transformation behaviour of two Ni-Mn-Ga alloys**, Zeitschrift für Metallkunde **95** (2004) 724-731.

III *A. Sozinov, A.A. Likhachev, N. Lanska, O. Söderberg, K. Koho, K. Ullakko, V.K. Lindroos,* **Stress-induced variant rearrangement in Ni-Mn-Ga single crystals with nonlayered tetragonal martensitic structure,** Euromech-Mecamat 7th European Mechanics of Materials Conference (EMMC7) Adaptive systems and materials: Constitutive Materials and Hybrid Structures, Frejus, France, May 18-23, 2003. Eds. C. Lexcellent and E. Patoor. Journal de Physique IV Proceedings **115** (2004) 121-128.

IV *A. Sozinov, A.A. Likhachev, N. Lanska, O. Söderberg, K. Ullakko, V.K. Lindroos,* **Stress- and magnetic-field-induced variant rearrangement in Ni-Mn-Ga single crystals with seven-layered martensitic structure**, ESOMAT'03 European Symposium on Martensitic Transformations and Shape-Memory Cirencester, England 17-22 August 2003. Ed. C. Friend. Materials Science and Engineering A **378/1-2** (2004) 399-402.

V *V.G. Gavriljuk, O. Söderberg, V.V. Bliznuk, N.I. Glavatska and V.K. Lindroos,* **Martensitic Transformations and Mobility of Twin Boundaries in Ni_2MnGa Alloys Studied by Using Internal Friction**, Scripta Materialia **49** (2003) 803-809.

VI *O. Söderberg, L. Straka, V. Novák, O. Heczko, S.-P. Hannula and V.K. Lindroos,* **Tensile/compression behavior of non-layered tetragonal $Ni_{52.8}Mn_{25.7}Ga_{21.5}$ alloy**, Materials Science and Engineering A **386** (2004) 27-33.

VII *A. Sozinov, A.A. Likhachev, N. Lanska, O. Söderberg, K. Ullakko and V.K. Lindroos***, Effect of crystal structure on magnetic-field-induced strain in Ni-Mn-Ga**, Smart Structures and Materials 2003: Active Materials: Behavior and Mechanics, 2003 2 – 6 March 2003, San Diego, California, USA. Ed. Dimitris C. Lagoudas, Proceedings of SPIE, **5053** (2003) pp. 586-594.

VIII *O. Söderberg, A. Sozinov and V.K. Lindroos* **Giant magnetostrictive materials.** In: J. Buschow (Ed.) The Encyclopedia of Materials: Science and Technology, Elsevier Science, 2004. *In press.*

BRIEF DESCRIPTION OF THE PUBLICATIONS

The present thesis collects and analyses the main results of the publications mentioned above. Their main results, in summary, are as follows:

PUBLICATION I, "*Composition and temperature dependence of the crystal structure in Ni-Mn-Ga alloys*", the results of a comprehensive study of the crystal structures in 33 different Ni-Mn-Ga alloys are collected. Several new compositions with ferromagnetic modulated martensitic crystal structure (**5M** or **7M**) yielding up to 353 K with their martensitic transformation region (T_M) and being good candidates for practical applications of MSM are presented. The evolution of the crystal parameters in different martensite types is shown as a function of the transformation temperatures. Furthermore, the non-modulated tetragonal martensite (referred as **NM** in *Publications I* and *III* and as **T** in the other publications) is the only possibility for the crystal structure in the martensitic alloys with $T_M > T_C$, while **5M** and **7M** structures, which are transformed straight from the parent phase, were observed only in the alloys $T_M < T_C$.

PUBLICATION II, "*Transformation behaviour of two Ni-Mn-Ga alloys"*, the transformation sequence of the alloy $Ni_{53.7}Mn_{26.4}Ga_{19.9}$ was confirmed to be $\mathbf{P_{param} \rightarrow T_{param} \rightarrow T_{ferrom}}$ in cooling with reverse reactions in respective order during heating, and for $Ni_{50.5}Mn_{30.4}Ga_{19.1}$ $\mathbf{P_{param} \rightarrow 7M_{param} \rightarrow 7M_{ferrom} \rightarrow T_{ferrom}}$ during cooling and $\mathbf{T_{ferrom} \rightarrow T_{param} \rightarrow 7M_{param} \rightarrow P_{param}}$ during heating. In this publication, it was for the first time suggested and confirmed that the hysteresis of Curie points during heating and cooling was due to the different magnetic transition temperatures of the **7M** martensite and the **T** martensite. Furthermore, the melting and solidification parameters together with the $\mathbf{L2_1 \rightarrow B2'}$ transition temperature were established for the studied alloys.

PUBLICATION III, "*Stress-induced variant rearrangement in Ni-Mn-Ga single crystals with nonlayered tetragonal martensitic structure"*, the transformation sequence of three Ni-Mn-Ga alloys were studied in detail. Two of the alloys showed the cubic parent phase to non-layered tetragonal phase transformation while in the third one the **T**-phase at ambient temperature was a result of an intermartensitic transformation (**7M**-**T**). X-ray diffraction, optical polarized microscopy and mechanical testing were used to study variant rearrangement in compression. A twinning strain of approximately 19 % was observed for all alloys. The temperature dependence as well as the influence of the magnetic field on the stress-strain curves is presented. It was found that the twinning stress in compression could not get below 6 MPa and, as the magnetically induced strain triggering the MSM effect was of a class 1 MPa, the alloys did not show detectable magnetic-field-induced strain.

PUBLICATION IV, "*Stress- and magnetic-field-induced variant rearrangement in Ni-Mn-Ga single crystals with seven-layered martensitic structure"*, presented four alloys showing cubic-**7M** martensitic transformation. It was confirmed that, if the structure was of pure **7M**, the low twinning stress (approximately 1-2 MPa) could be reached by successive compressions. Consequently, these alloys showed the magnetic-field-induced strain of approximately 10 % at ambient temperature in a magnetic field of the order of 1 T (approximately 800 kA/m). The temperature dependence of the twinning stress was studied as well as the influence of the magnetic field on the stress-strain curves.

PUBLICATION V, "*Martensitic transformations and mobility of twin boundaries in Ni_2MnGa alloys studied by using internal friction*", the internal friction (IF) was measured in two non-stoichiometric Ni_2MnGa alloys with non-modulated martensite (**T**) structure. From the strain dependence of IF, the activation enthalpy for the movement of twin boundaries between martensitic domains was estimated to be equal to 0.02-0.04 eV. The temperature dependence of the internal friction, i.e. twin-boundary mobility, was confirmed for the studied alloys.

PUBLICATION VI, "*Tensile/compression behavior of non-layered tetragonal $Ni_{52.8}Mn_{25.7}Ga_{21.5}$ alloy*", showed the total strain of the **T** martensitic alloy during one tensile-compression cycle to be 21-22 % while the detwinning stress could be decreased from the 18-20 MPa value at the beginning to about 10-12 MPa after some cycles. It was suggested that the shape variations of approximately 15 % during tension and approximately 7 % during compression were due to the maximum crystallographic changes of the two martensite single-variant states, in between which the material altered during the cycling. The single-variant state of the material after the tensile load was confirmed by the X-ray method. The effect of temperature on the tensile/compression behaviour was also studied and it was confirmed that, in the vicinity of the reverse transformation to the parent phase, the detwinning stress approached 6.7 MPa.

PUBLICATION VII, "*Effect of crystal structure on magnetic-field-induced strain in Ni-Mn-Ga*", gives a comprehensive overview of the crystal structures, magnetic anisotropy and twinning stress of the martensitic phases in Ni-Mn-Ga alloys. The most important experimental results are reported on the alloys having tetragonal five-layered, orthorhombic seven-layered and tetragonal non-layered structures. Depending on the martensite crystal structure, Ni-Mn-Ga alloys are able to show a really giant strain response (approximately 6 % in tetragonal five-layered or 10 % in orthorhombic seven-layered martensitic phase) in a magnetic field less of than 1 T (approximately 800 kA/m). However, a detectable field-induced strain is not observed in the non-layered tetragonal martensitic phase in the Ni-Mn-Ga system. The effect of the crystal structure is in good agreement with the calculation of the magnetic-field-induced strain, based on the model requiring the magnetically induced stress to be larger than the twinning stress.

PUBLICATION VIII, "*Giant magnetostrictive materials*", gives an overview of the magnetic shape memory effect, its principles and the major material groups presenting it.

AUTHORS CONTRIBUTION

All publications were carried out within the HUT-MSM project. Two of the publications were also funded by the co-operative projects of the Academy of Finland: *Publication V* with the Institute for Metal Physics Kiev, Prof. Gavriljuk's research group, and *Publication VI* with the Institute of Physics, Prague, with Dr. Novák. The author was responsible for the selection of the studied Ni-Mn-Ga materials of the publications. In the HUT-MSM project she was responsible for the total material characterization (chemical analyses, transformation and magnetic transition temperatures). Certain parts of the material characterization were carried out by others as explained below, while the author took care of the transformation characterization of the alloys with Linkam differential scanning calorimeter DSC and optical methods. The author is reponsible for these results in all of the *Publications*. The author participated in the writing process of all the *Publications* and is the responsible author of *Publications II, VI* and *VIII*. The co-authors of the *Publications* have contributed the following parts:

- **Prof. Veikko Lindroos** was the HUT-MSM project leader.
- **Prof. Simo-Pekka Hannula** was the leader of the work carried out after 1st Jan. 2004.
- **Dr. Kari Ullakko** was the scientific leader of the HUT-MSM project.
- **Dr. Alexei Sozinov** led the work carried out with the MSM-alloy magneto-mechanical testing and development.
- **Dr. Oleg Heczko** led the work carried out with the magnetic properties of the alloys as well as the magnetic measurements.
- **Dr. Alexander Likhachev** created the theoretical macroscopic models for MSM behaviour.
- **Nataliya Lanska** M.Sc. was responsible for the characterization of the crystal lattices of the alloys with the X'pert equipment.
- **Ladislav Straka** M.Sc. took care of the magnetic measurements and equipment as a part of his post-graduate studies.
- **Yanling Ge** M.Sc. was responsible for the SEM-EDS/WDS-analysis of the alloys as well as their study with different SEM-methods and X-rays as a part of her post-graduate studies.
- **Kari Koho** M.Sc. carried out the mechanical testing of the alloys in his master's degree thesis and later on with the quaternary Ni-Mn-Ga based alloys.
- In the co-project with the Laboratory of Materials Processing and Powder Metallurgy, **Michael Friman** M.Sc., together with **Dr. Marko Hämäläinen**, carried out the work and the analysis of the measurements with the Netzsch DSC equipment.
- The internal friction studies and their analyses were carried out by **Prof. Gavriljuk**, **Dr. Bliznuk** and **Dr. Glavatska** at the Institute for Metal Physics, Kiev.
- The tensile/compression experiments were carried out by **Dr. Novák** and **Ladislav Straka** M.Sc. at the Institute of Physics, Prague.

SYMBOLS AND ABBREVIATIONS

Ni	nickel, in the alloys as atomic-%
Mn	manganese, in the alloys as atomic-%
Ga	gallium, in the alloys as atomic-%
Heusler alloy	chemical composition of X_2YZ
e/a	the average number of valence electrons per atom
bcc	body centered cubic crystal lattice
a, b, c	crystal lattice parameters in the cubic parent phase coordinates
a_m	lattice parameter *a* of the martensite
a_p	lattice parameter *a* of the parent phase
b_m	lattice parameter *b* of the martensite
c_m	lattice parameter *c* of the martensite
a_{ort}, c_{ort}	lattice parameters in the orthorhombic coordinates
a-axis, *b*-axis, *c*-axis	correspondent crystallographic axis in the cubic parent phase coordinates
α, β, γ	angles between crystallographic axes
c/a	ratio of the lattice parameters *a* and *c*
B2'	the disordered high temperature phase of Ni-Mn-Ga
$L2_1$, P, A	the ordered cubic parent phase of Ni-Mn-Ga
P_{param}	the paramagnetic cubic parent phase
P_{ferrom}	the ferromagnetic cubic parent phase
M	a martensite phase
IM	an intermartensitic phase
M_1	a modulated martensite with *c/a* <1, ref. [89]
M_2	a non-modulated martensite with *c/a* >1, ref. [89]
5M	the five layered tetragonal or slightly monoclinic martensite
7M	the seven layered orthorhombic or slightly monoclinic martensite
$7M_{param}$	the paramagnetic **7M** martensite phase
$7M_{ferrom}$	the ferromagnetic **7M** martensite phase
T, NM	the non-modulated tetragonal martensite
T_{param}	the paramagnetic **T** martensite phase
T_{ferrom}	the ferromagnetic **T** martensite phase
8M, 10M	modulated martensite structures, modulation according to number, ref. [88]
T	temperature in Kelvins (K)
$T_{ambient}$	ambient temperature, i.e. room temperature (K)
M_s	the start temperature of the martensitic transformation (K)
M_f	the finish temperature of the martensitic transformation (K)
A_s	the start temperature of the reverse transformation (K)
A_f	the finish temperature of the reverse transformation (K)

$M_{s\mathbf{7M\rightarrow T}}$	the start temperature of the intermartensitic transformation **7M→T** (K)
$M_{f\mathbf{7M\rightarrow T}}$	the finish temperature of the intermartensitic transformation **7M→T** (K)
$A_{s\mathbf{T\rightarrow 7M}}$	the start temperature of the reverse intermartensitic transformation **T→7M** (K)
$A_{f\mathbf{T\rightarrow 7M}}$	the finish temperature of the reverse intermartensitic transformation **T→7M** (K)
T_o	the martensite transformation temperature, ½ (M_s + A_f) (K)
T_M	the average of all transformation temperatures ¼ (M_s + M_f + A_s + A_f) (K)
T_M	the martensite transformation average temperature, ½ (M_s + M_f) (K) [applied in *Publication I*]
T_C	the Curie point in Kelvins (K) – temperature at which the magnetic transition between the paramagnetic and ferromagnetic state takes place
$T_{C\mathbf{M}}$	the Curie point of a tetragonal martensite **M** (K)
$T_{C\mathbf{P}}$	the Curie point of the parent phase **P** (K)
T_{Ch}	the Curie point during heating of the alloy (K)
T_{Cc}	the Curie point during cooling of the alloy (K)
$T_{C\mathbf{7M}}$	the Curie point of the **7M** martensite phase (K)
$T_{C\mathbf{T}}$	the Curie point of the **T** martensite phase (K)
σ_{tw}	twinning stress, the critical stress needed for the twin-boundary motion, i.e. twin variant rearrangement, indicated with stress-plateau in a stress-strain curve
ε_0	the maximum strain associated to the twinning stress, i.e. the maximum deformation of the structure
σ_{mag}	the magnetic field induced stress
MFIS	a magnetic field induced strain (%)
MSM	magnetic shape memory
MSME	magnetic shape memory effect
FSMA	ferromagnetic shape memory alloys
H	magnetic field in SI-unit kA/m (800 kA/m ~ 1 Tesla)
K_U	the magnetic crystallographic anisotropy in J/m^3
K_a, K_b	the magnetic anisotropy constants to the given axis directions in J/m^3
K_1, K_2	the magnetic anisotropy constants in **T** martensite in J/m^3
E_A	the magnetic anisotropy energy in J/m^3
Q^{-1}	the internal friction

TABLE OF CONTENTS

ABSTRACT iii

FOREWORD iv

LIST OF PUBLICATIONS I-VIII vi
Brief description of the publications vii
Author's contribution ix

SYMBOLS AND ABBREVIATIONS x

TABLE OF CONTENTS xii

1. INTRODUCTION 1
   1.1. General introduction 1
   1.2. Objectives and scope of the study 1
2. Ni-Mn-Ga ALLOYS 2
   2.1. High-temperature phases of Ni-Mn-Ga 3
   2.2. Martensites in Ni-Mn-Ga system 3
      2.2.1. Martensite transformations in Ni-Mn-Ga 4
      2.2.2. Martensitic structures 5
   2.3. The Curie point 7
3. DETWINNING OF THE Ni-Mn-Ga ALLOYS 8
   3.1. Detwinning 8
4. MAGNETIC SHAPE MEMORY EFFECT 9
   4.1. Magneto-mechanical stress requirement for MSME 11
5. EXPERIMENTAL METHODS 12
6. CRYSTAL STRUCTURES OF THE STUDIED ALLOYS AT AMBIENT TEMPERATURE 12
7. TRANSFORMATION SEQUENCES IN SELECTED ALLOYS 14
8. MECHANICAL BEHAVIOUR OF THE SELECTED ALLOYS 22
9. MAGNETO-MECHANICAL BEHAVIOUR OF SELECTED ALLOYS 28
10. CONCLUSIONS 31

LIST OF REFERENCES 32

PUBLICATIONS 40

APPENDIX A A1

1. INTRODUCTION

The aim of the present work is to advance the Ni-Mn-Ga alloys towards the magnetic shape memory applications at elevated temperatures. The basis of this are the alloys with the ferromagnetic twinned martensitic crystal structure showing the high magnetocrystalline anisotropy, relatively high transformation temperatures and the low stress of the twin-variant rearrangement.

1.1. General introduction

The term “smart” or “intelligent” material is usually used in the context of adaptive structures having sensing, control and actuation capabilities [1-3]. These structures respond to changes of the surrounding environment such as external loads, altering temperature, electrical or magnetic fields, humidity or to internal changes such as damage or failure. Smart materials possess potential to embody the function of a smart structure. They may achieve several functions such as sensor, processor, actuator (effector) and feedback-forward. It is generally required that the intelligent material performs multifunctionally, i.e. it possesses at least two or three of these attributes, for example, simultaneously as sensors and actuators.

An ideal material for actuator-sensor applications has a high-frequency response with large-strain and high-force production under precise control. So far, a single material that exhibits all these features is not available. In actuator applications based on smart materials, the electrically driven piezoelectric materials, magnetically controlled magnetostrictive materials and the thermally activated shape memory alloys have been utilized [1,4,5]. The obtainable strains in the first two groups are comparably small, while the third group has a relatively slow working frequency. The magnetic shape memory (MSM) alloys, also referred to as ferromagnetic shape memory alloys (FSMAs), produce a large strain with rather high frequencies without a change in the external temperature [6]. So far, the best working MSM materials are based on Ni-Mn-Ga alloys [7-22]. In these, the MSM phenomenon has been demonstrated in two of the martensitic structures with the phase transformation close to the ambient temperature.

1.2. Objectives and scope of the study

As the aim of the present thesis is to seek Ni-Mn-Ga alloys for the magnetic shape memory applications at elevated temperatures, where the main focus is given to the high-temperature alloys showing the 7-layered near-orthorhombic martensite structure (**7M**) and the non-modulated tetragonal martensitic (**T**) alloys. The currently best working Ni-Mn-Ga MSM alloys have usually a 5-layered modulated tetragonal (**5M**) crystal structure with the phase transformations up to 333 K.

The literature review of the present work gives an overview of the Ni-Mn-Ga alloys, their crystal structures and their behaviour, as well as of the principles of MSME. The basic requirement for the MSME is presented as follows: the magnetically induced stress must exceed the stress needed for the rearrangement of the twin structure, i.e. twinning stress, both of which are characteristic of the particular crystalline structure.

The experimental results present 37 Ni-Mn-Ga alloys including, especially, some new alloys with the **7M** structure. The transformation sequences of the **7M** and the **T** phases are studied in more detail in order to establish the possible service temperatures of MSME. The studied alloys are also classified according to their magneto-crystalline transformation behaviour. The hysteresis of the Curie point connected to the co-occurrence of the magnetic transition and the double-step martensitic/reverse reaction revealed the Curie point of the 7M martensite ($T_{C\mathbf{7M}}$).

With mechanical testing, the pre-straining procedures for obtaining the single-variant state in the **7M** and **T** martensite are introduced. The mobility of the twin boundaries in the **T** phase is established by means of the internal friction measurements. The magneto-mechanical experiments confirm the postulation that the MSME is possible in the **7M** structure in which the magnetically induced force exceeds the twinning stress. It is also shown that in the **T** phase this is not the case and, consequently, the magnetic shape memory effect is not possible in it.

2. Ni-Mn-Ga ALLOYS

The Ni-Mn-Ga alloys have been already studied for approximately 40 years when the work exhibiting Ni_2MnGa alloy as one of the Heusler alloys having the formula X_2YZ [5,23-28] is included. The first copper-manganese-based Heusler alloys, discovered by Heusler, Starck and Haupt [23], were unique, since they were ferromagnetic whereas their constituent elements were not. Soltys was the first to concentrate only on this alloy system [29,30]. The martensitic transformation in Ni_2MnGa at low temperatures was discovered by Webster *et al.* [31]. More systematic studies, the work carried out by Kokorin *et al.* [32,33], for example, and by Chernenko *et al.* [34] was initiated in the early 1990's as Ni-Mn-Ga alloys were investigated as potential shape-memory alloys. After Ullakko *et al.* [9] had demonstrated the magnetically induced strain (MFIS) in a Ni-Mn-Ga single crystal, a totally new era of investigations started. The Ni-Mn-Ga alloys have now been studied in more detail by different researchers and it has been established that the martensitic and magnetic transformation temperatures [35-40], transformation enthalpy [36,37], magnetocrystalline anisotropy [40] and saturation magnetization [39,40] are highly composition dependent. Consequently, certain important properties of Ni-Mn-Ga have been mapped together with their composition [40,41].

2.1. High-temperature phases of Ni-Mn-Ga

As the behaviour of the materials depends on their thermal history, it is important to study the details of the solidification process and heat treatments. This is especially crucial in the Ni-Mn-Ga alloys in which the material properties are extremely composition dependent. Schlagel *et al.* [42] as well as Wedel and Itakagi [43] studied the solidification. Soltys [30], Overholser *et al.* [44] and Khovailo *et al.* [45] investigated the high-temperature ordering of Ni-Mn-Ga alloys. Schlagel *et al.* [42] studied the solidification process of Ni-Mn-Ga alloys and confirmed that the solidified materials possess a great inhomogeneity. Ni-Mn-Ga alloys solidify to a partially disordered intermediate phase **B2'**, in which the Ni atoms form the frame of the lattice while Mn and Ga atoms are situated arbitrarily [5,44]. Wedel and Itakagi [43] found that this single-phase cubic structure exists in a broad range of Ni-Mn-Ga compositions. $Ni_{45}Mn_{55-x}Ga_x$ alloys, for example, have the cubic structure ($Pm\bar{3}m$ or **B2'**) at 1073 K for all *x* values from 0 to 55. According to Overholser *et al.* [44], this crystal structure transforms to Heusler type ($Fm\bar{3}m$ or $\mathbf{L2_1}$) at a particular composition-dependent temperature. For the stoichiometric Ni_2MnGa alloy, this structure appears below 1071 K. According to Khovailo *et al.* [45], the conversion $\mathbf{B2' \rightarrow L2_1}$ is a second-order phase transition of the disorder-order type. The first-order phase transition, i.e. the martensitic reaction, takes place at much lower temperatures.

Kreissl *et al.* [46] studied the effect of the high-temperature structure ordering on the martensitic transformation. The martensitic transformation is suppressed down to 100 K in the Ni_2MnGa alloy with the disordered **B2'** structure from 200 K obtained with the ordered $\mathbf{L2_1}$ structure. Tsuchiya *et al.* [47] and Pasquale *et al.* [48,49] have confirmed that with the ordered $\mathbf{L2_1}$ structure obtained in the correct annealing procedure the martensitic transformation temperature region is narrower. The annealing procedure also affects both the martensite transformation temperature and the Curie point.

The ordered $\mathbf{L2_1}$ structure of the cubic parent phase (**P**) can be represented with a *bcc* lattice in which the Ni atoms are in the positions at the centre of the cube and Mn as well as Ga atoms occupy alternatively the positions at the apexes [5,31]. For the stoichiometric Ni_2MnGa alloy, the cubic lattice constant at ambient temperature is 0.5825 nm, but since the cubic structure is stable down to 202 K it should be noted that this value is temperature dependent [5,31,35]. In addition to the temperature dependency, the lattice constant is also composition dependent. For the alloy $Ni_{51.2}Mn_{31.1}Ga_{17.7}$, for example, the cubic lattice constant is 0.583 nm [50], while for the alloy $Ni_{51.1}Mn_{28.4}Ga_{20.5}$ a value of 0.5837 nm is measured at 373 K [51]. The cubic parent phase is much stronger than the martensitic structures [52,53]. The magnetic anisotropy of the cubic phase is much lower than that of the martensitic structures and the magnetization saturates at H = 160 kA/m [35]. In the stoichiometric alloy, the Curie point of the cubic phase is 376 K [35].

2.2. Martensites in Ni-Mn-Ga system

The Ni-Mn-Ga alloys show a variety of different martensitic structures. The crystal structure of the martensite depends strongly on the chemical composition as shown by Chernenko *et al.* [34,36,50], Pons *et al.* [54] and Tsuchiya *et al.* [55]. When the possibility of the MSM effect is studied in Ni-Mn-Ga alloys, the main interest is focussed on the ferromagnetic twinned martensite structures.

The crystal structure of martensite is an important factor that affects the magnetic anisotropy and behaviour [56-58] as well as the mechanical properties of Ni-Mn-Ga alloys [for example, 57-59] and the chemical behaviour [60,61]. The martensitic structures, transformation temperatures and the Curie points have been systematized as functions of the average number of valence electrons per atom (*e/a*) [36,39,54,55]. This approach was introduced by Chernenko *et al.* [36], who calculated the electron concentration using the electron concentration of the outer shells for each chemical component of the Ni-Mn-Ga alloy as follows:

$$e/a = \frac{10x(Ni_{at\%}) + 7x(Mn_{at\%}) + 3x(Ga_{at\%})}{(Ni_{at\%} + Mn_{at\%} + Ga_{at})} \qquad (1)$$

Here, the value of 10 is applied for nickel, in which the outer electron shells are occupied as $3d^8 4s^2$, while for manganese the value becomes 7 from $3d^5 4s^2$ and for gallium 3 from $4s^2 4p^1$.

2.2.1. Martensite transformations in Ni-Mn-Ga

The martensite reaction is a diffusionless solid state phase transformation in which a short-range atom shift occurs over a certain temperature region usually showing hysteresis between the forward and reverse reactions [1,5,62]. The chemical composition of the alloy does not change. The parent and the martensite phases have a clear correspondence with the crystal structures. Martensite reaction is usually accompanied by large heat and volume effects [5]. The shape change is accommodated either by plastic slipping of the dislocations or by twinning, i.e. a mirror-like stacking fault of the closest packed atom layers [1]. The hysteresis and the large heat effects are due to the increase of the elastic and the surface energies during the martensite formation. When the new phase grows inside the parent phase, energy is stored to the structure. During reverse transformation, this stored energy is released, usually at temperatures higher than those at which it was stored. If the stored energy is small, the hysteresis is narrow and the interface between the parent and martensite phases is very mobile upon cooling and heating [1]. Twinning can carry out the accommodation of the intrinsic transformation strain of the martensitic transformation totally, if the elastic modulus of the phases is small and their elastic limit is high [5]. Here, the parent phase structure can be restored in the reverse transformation. This thermoelastic martensite transformation is a requirement for the shape memory effect and superelasticity, as well as for the magnetic shape memory effect [5,19].

Supercooling is necessary for the nucleation of the martensite and, consequently, the martensitic reaction is usually athermal with the particular temperatures for the start of the martensite formation (M_s) and the finish of it (M_f). In the reverse transformation, while martensite transforms back to the parent phase during heating, the parent-phase formation starts at temperature A_s, and finishes at temperature A_f. The transformation region can be characterized by the martensite transformation temperature $T_o = ½ (M_s + A_f)$ [1]. In the thermodynamical calculations, T_o refers to the temperature at which the Gibbs energies of the martensitic and parent phases are equal [63].

The transformation temperatures of martensites in the Ni-Mn-Ga alloys depend strongly on the chemical composition: both the deviation from the stoichiometry [for example, refs. 19,34,35,37-39,41,49,54,55,64-69] and the doping with other elements [for example, refs. 36,51,70-79]. Chernenko *et al.* [34] conclude that the Ga addition in $Ni_{2-x}MnGa_{1+x}$ alloys and the Mn increase in $Ni_{2-x}Mn_{1+x}Ga$ alloys decrease the M_s temperature. In $NiMn_{1+x}Ga_{1-x}$ alloys, the higher Mn content raises the M_s value. This is in accordance with Wirth *et al.* [64] and with Dikhstein *et al.* [66], who show that the martensitic transformation temperature increases with Ni content in the alloys $Ni_{2+x}Mn_{1-x}Ga$ (x = 0-0.2). Ezer [19] shows that the M_s temperature increased with the increasing ratio of Mn/Ga. According to these studies, one may suggest that increasing the Ni content and increasing the Mn/Ga while keeping the Ni amount fixed, should result in the higher martensite transformation temperature. Jin *et al.* [39] describe the increase of the martensite transformation temperature as a linear function with the *e/a* concentration.

In the stoichiometric Heusler Ni_2MnGa alloy, the martensitic reaction at approximately 200 K leads to a modulated tetragonal martensite with lattice parameters $a = b =$ 0.5920 nm and c = 0.5566 nm [31]. However, several other martensite structures also exist in the Ni-Mn-Ga system. The most important of them are the five layered tetragonal martensite (**5M**), the seven layered near-orthorhombic martensite (**7M**) and the non-modulated tetragonal martensite (**T**) [5,6]. Which of them appears during cooling depends on the composition of the alloy and the thermal stability of the different martensitic phases. There seems to be a certain order according to which they emerge in the martensite reaction or change in the intermartensitic transformations. This has been described schematically by Enkovaara and Sozinov [80]. The **T** structure is the most stable one of the three martensite phases [57,69,80,81] and the alloys transforming straight to the **T** martensite from the parent phase have typically transformation temperatures close or above the Curie point [34,35,37,54,80-89]. The **5M** structure transforms directly from the parent phase at lower temperatures close to the ambient one, while the **7M** martensite appears directly from the parent phase only in a narrow temperature range below the Curie point [22,80]. The transformation to the stable non-modulated martensite with $c/a>1$ can also take place via the intermartensitic reactions such as **P→M$_1$→M2, P→8M(10M)→T** or **P→5M→7M→T** [87-90]. Chernenko *et al.* [88] showed that the ratio of the transformation enthalpies is 10:1 in the sequence **P→8M(10M)→T**. Due to the change in the crystal structure, the intermartensitic reaction (IM) seems to set the lowest service temperature for the magnetic shape memory effect (MSME) [91].

2.2.2. Martensitic structures

The crystal structure of Ni-Mn-Ga martensites strongly depends on composition and temperature. A correlation between the average number of valence electrons per atom (*e/a*) of Eq. (1) and the tetragonal distortion of the cubic lattice caused by the martensite reaction expressed with the ratio of the lattice parameters has been suggested [36,50,54,55]. The lattice parameters can be given in the so-called orthorhombic coordinates in which the axes are parallel to the diagonal directions of the cubic coordinates [54]. This approach is convenient in the description of the crystal lattice modulation as a long-period superstructure. However, for a simple description of the strain values induced by stress or magnetic field, the cubic parent phase coordinates are

more practical [4]. Consequently, in the present work the lattice parameters refer to the cubic parent phase coordinates. The correlation of the lattice parameters of these different coordinate systems given by Pons *et al.* [54] is

$$a = \frac{a_{ort}}{\sqrt{2}} \text{ and } c = c_{ort} \qquad (2)$$

where a and c refer to the lattice constants given in the cubic parent coordinates and a_{ort} and c_{ort} are the parameters in the orthogonal coordinates.

When applying the cubic coordinate system, the modulated structures **5M** and **7M** have a lattice parameter ratio $c/a<1$ and in the non-modulated tetragonal **T** martensite $c/a>1$. Chernenko *et al.* [50] showed that the change of the c/a to values above 1 takes place at $e/a = 7.7$. Tsuchiya *et al.* [55] estimated this critical value to be 7.61-7.62. In both cases, the observed change has been based on the data of the **T** martensite, while no data for the **7M** was used and the alloys with **5M** structure showed martensitic phase transformation below ambient temperatures.

5M martensite

The **5M** martensite was first discovered by Webster *et al.* [31] in the stoichiometric Ni_2MnGa alloy. Martynov and Kokorin [81,82] and Fritsch *et al.* [92] discovered that the crystal structure is modulated by a transverse displacive wave along the [110] direction. This may be presented as a periodic suffling along $(110)[110]_p$ system or a long-period stacking of $\{110\}_p$ close-packed planes [54,81]. The modulation can be observed in neutron, electron or X-ray diffraction measurements as four additional spots between the main reflections along the [110]* direction in the reciprocal space (for example, [93,94]). The average lattice is approximately tetragonal or monoclinic with a short c-axis, with ratio $c/a<1$ (the cubic coordinates). The effect of temperature on the lattice parameters in the stoichiometric Ni_2MnGa alloy has been studied by Ma *et al.* [95], while Glavatska *et al.* [94,96] studied a working MSM alloy with the **5M** structure. They discovered that the tetragonality of the martensitic lattice increases with decreasing temperature and saturates at very low temperatures. The short c-axis is also the easy axis of magnetization [8]. The saturation magnetization of 64.2 Am^2/kg for the **5M** alloy $Ni_{50.7}Mn_{28.4}Ga_{20.9}$ is given by Heczko *et al.* [56]. At the ambient temperature, the magnetic anisotropy of the **5M** martensite may have values in the range $K_U = 1.45…1.67 \times 10^5$ J/m^3, depending on the alloy composition [12,13,56,57]. K_U is fairly stable from very low temperatures close to the reverse transformation region, when it decreases quickly [91,97,98].

7M martensite

Martynov and Kokorin [81,82] found the **7M** martensite. The average lattice is approximately orthorhombic with $c/a \approx 0.89$ and $c/a<1$ (in cubic coordinates) with a monoclinic distortion of less than 0.4^o, as observed by Sozinov *et al.* [99]. In the orthorhombic coordinates, the lattice of the **7M** martensite is seen as a monoclinic one with $\beta \approx 93\text{-}94^o$ [54]. The **7M** martensite gives in diffraction studies a pattern where the distance between the main reflection along [110]* direction in reciprocal space is divided into seven parts by six additional spots, as shown by Fritsch *et al.* [92], Ge *et al.* [93] as well as by Lanska and Ullakko [100]. Sozinov *et al.* [22] observed that the seven-layer modulation took place along the $(110)[1\bar{1}0]_p$ system. They established that in the **7M** martensite the easy axis of magnetization is the shortest c-axis, while the longest a-axis is the hardest to magnetize and the magnetization of the b-axis is the

intermediate one. Consequently, two magnetic anisotropy constants K_b and K_a are needed to characterize the orthorhombic crystal structure. At ambient temperature, for the alloy $Ni_{48.8}Mn_{29.7}Ga_{21.5}$, the values of $K_b = 0.7 \times 10^5$ J/m^3 and $K_a = 1.6 \times 10^5$ J/m^3 are given [22], while for the alloy $Ni_{50.5}Mn_{29.4}Ga_{20.1}$, the obtained values were $K_b = 1.02 \times 10^5$ J/m^3 and $K_a = 1.74 \times 10^5$ J/m^3 [56]. Heczko *et al.* [56] give the saturation magnetization 60.3 Am^3/kg for the alloy $Ni_{50.5}Mn_{29.4}Ga_{20.1}$.

Non-modulated T martensite

The non-modulated **T** martensite of the Ni-Mn-Ga system was also found by Martynov and Kokorin [81]. The crystal structure is tetragonal with a long *c*-axis and $c/a > 1$ (in cubic coordinates). According to [50,54], the change from $c/a < 1$ to $c/a > 1$ takes place when $e/a \geq 7.7$. Since the **T** phase is the most stable one of the martensitic structures in Ni-Mn-Ga alloys, it can exist at very low temperatures as a last transformation product of intermartensitic reactions, but it is also the only martensitic phase that exists at elevated temperatures and above T_C [34-37,54,64,80-88,90,101-103]. The magnetic anisotropy of the **T** phase is higher than the one of the **5M** and **7M** martensites [56,57,97]. Since in this structure the long *c*-axis is the axis of hard magnetization and the shorter *a*- and *b*-axis are easily magnetized, the ferromagnetic **T** martensite has an easy plane of magnetization [56-58,97]. At ambient temperature, the magnetic anisotropy constants for the easy and hard magnetization axes of the alloy $Ni_{50.5}Mn_{30.4}Ga_{19.1}$ are $K_1 = -2.3 \times 10^{-3}$ J/m^3 and $K_2 = 0.55 \times 10^{-3}$ J/m^3 [97]. The total sum of these two, -1.45×10^{-3} J/m^3, coincides well with the area between the magnetization curves for easy and hard directions [97]. According to ref. [56], the magnetic anisotropy energy is $E_A = 1.44 \times 10^5$ J/m^3. For the alloy $Ni_{52.1}Mn_{27.3}Ga_{20.6}$, the value of $K_U = -2.03 \times 10^5$ J/m^3 is given [57]. The non-modulated tetragonal **T** structure seems to possess the best chemical properties among the Ni-Mn-Ga martensites [60,61]. Its corrosion resistance in artificial seawater was higher than the one of the **7M** and **5M** martensites. Generally, the studied Ni-Mn-Ga alloys tolerated the artificial seawater better than the common low-alloyed steel, but not as well as the AISI316L stainless steel.

2.3. The Curie point

At the Curie point (T_C), a ferromagnetic material becomes paramagnetic by loosing the long-range magnetic order. This magnetic transition is one of the main limits when considering the service temperatures of the MSM effect. The magnetic moment of Ni-Mn-Ga alloys originates mainly from Mn having the largest magnetic moment, while the small magnetic moments of the Ni sites are also confined to it [31]. The calculations in [80] show that the excessive Mn atoms may couple antiferromagnetically to their neighbouring Mn atoms and, thus, decrease of the effect of Mn alloying on the magnetic moment. In this case, the Ni content is important in determining the Curie temperature. It is suggested that the profound magnetic moment at the Ni sites is correlated with a low Curie temperature.

Chernenko *et al.* [50] and Tsuchiya *et al.* [55] have shown that in Ni-Mn-Ga alloys with $e/a < 7.6$-7.62 the martensitic transformation takes place below T_C, while in the alloys with $e/a > 7.62$-7.7 the structural transition occurs in the paramagnetic state. The co-occurrence of the structural and magnetic transitions has recently been studied more, due to the possibility of the magnetocaloric effect. It could be applied to the magnetic-field-controlled heat production [104]. Chernenko *et al.* [50], as well as

Khovailo *et al.* [105], have studied in more detail the magnetic transition of the Ni-Mn-Ga alloys. They suggested that the cubic parent phase and the tetragonal martensitic phase both have their own Curie points with an approximately 30 K difference. The Curie point of the low-volume tetragonal martensite ($T_{C\mathbf{M}}$) was higher than the one of the high-volume cubic parent phase ($T_{C\mathbf{P}}$). In addition to the different lattice volumes, the different Curie points were explained by the dissimilar Mn-Mn atom distances and the different electronic structures.

3. DETWINNING OF THE Ni-Mn-Ga ALLOYS

The current work presents the mechanical behaviour of the studied materials only in the stress-region needed for moving the twin boundaries. This information is needed, since the magnetic shape memory effect (MSME) is based on the rearrangement of the twin variants by the twin-boundary motion. The rearrangement is the same as obtained in the detwinning when the conventional shape memory alloys are mechanically deformed.

3.1. Detwinning

The thermally formed martensitic twin structure is usually very complex. For example, a tetragonal structure may consist of twelve different larger habit plane variants (HPV), each of which can be formed from six different lattice correspondence variants (LCV) [1]. In detwinning, those martensite twin variants that are favourably oriented towards the applied force grow at the expense of the other martensite variants [1]. The detwinning starts when a certain critical stress is exceeded. This critical stress corresponds to the force needed for the twin-boundary motion and it is referred to as the twinning stress, σ_{tw}, in studies of the MSME. As the detwinning continues, the amount of the different variants in the structure decreases so that, in the end, the whole structure is of one variant, i.e. it is in single-variant state. This procedure is indicated by a stress-plateau of the stress-strain curve [1] and the maximum strain associated with it depends on the crystal lattice distortion of the structure. This maximum strain (ε_0) can be given as a function of the lattice parameter ratio as follows

$$\varepsilon_0 = \left| 1 - c/a \right| \qquad (3)$$

where *c* and *a* are lattice parameters of martensite (the cubic coordinates) [4]. In the modulated structures (**5M** and **7M**), the maximum strains are about 6 % and 10 %, while in the non-modulated **T**-structure it is approximately 20 % [12,13,15,22,57,59,86]. The twinning stress in compression varies from less than 2 MPa of the **5M** and **7M** structures to the 18-20 MPa of the **T** martensite. The behaviour of different martensite types is shown in Figure 1, where the detwinning of the martensite phases of one alloy ($Ni_{50.6}Mn_{28.5}Ga_{20.9}$) is measured at the characteristic temperatures related to them. The detwinning of the structure in correlation to the stress-strain curve is shown schematically in the insert.

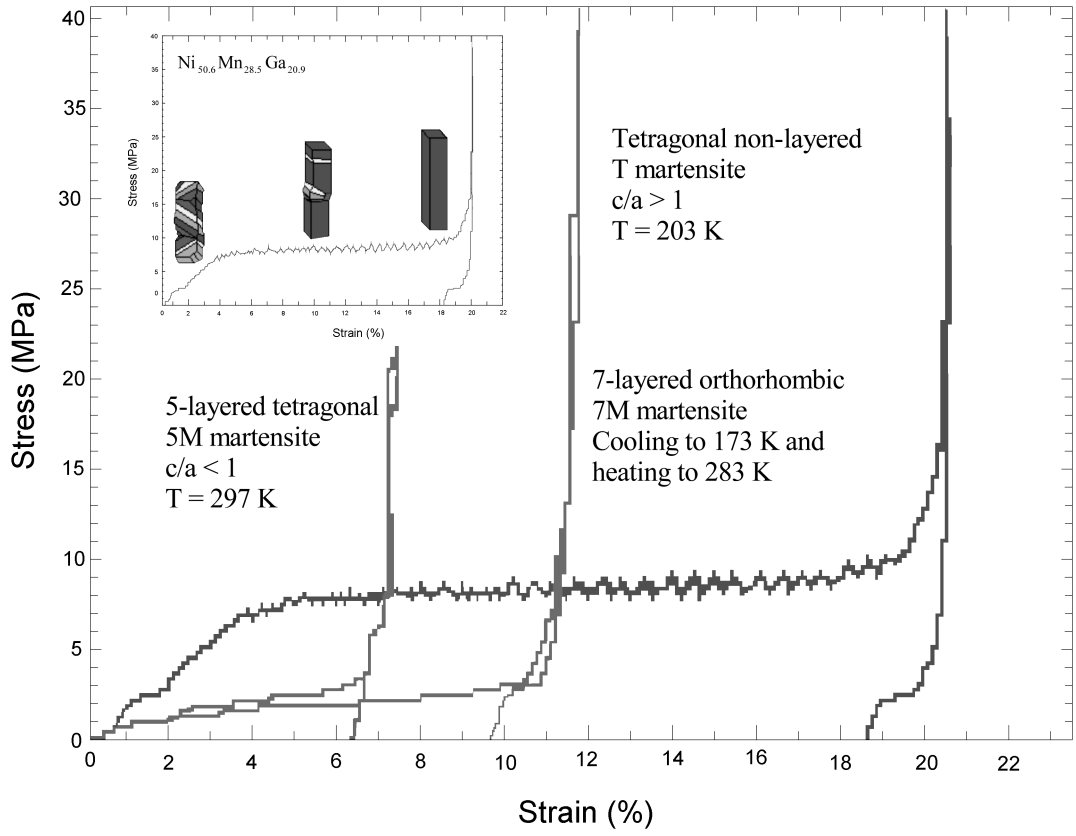

Figure 1. The stress-strain curves in compression of the alloy $Ni_{50.6}Mn_{28.5}Ga_{20.9}$ at different temperatures. The crystal structure changes from the **5M** martensite at ambient temperature to the **7M** structure after cooling to 173 K and then heating up to 283 K and finally to the **T** martensite 203 K. The detwinning and the stress plateau connected to it are shown schematically in the insert. [Results obtained in the HUT-MSM project in the studies connected to the ref. 90].

4. MAGNETIC SHAPE MEMORY EFFECT

The magnetic shape memory effect (MSME) is based on the rearrangement of the martensitic crystallographic domains (twin variants) in an applied magnetic field. As in the mechanically induced detwinning, the maximum magnetic-field-induced strain (MFIS) can be 6 % (**5M**) or 10 % (**7M**) depending on the crystal structure and the applied field [see, for example, 4,5,13,15,22,57]. The rearrangement of the twin variants lowers the magnetization energy [9]. Since MSME works in certain kinds of ferromagnetic twinned martensites, it is possible only at temperatures below the Curie point (T_C) and below the reverse transformation (A_s). The minimum of the MSME operating temperature is set either by the intermartensitic transformation **5M**→**7M** [94,106] or **7M**→**T** [22] or by the twinning stress, which increases with cooling [59] and exceeds the magnetic force at very low temperatures [106]. The critical material parameters for MSME are the magnetocrystalline anisotropy (K_U), the saturation

magnetization and the twinning stress (σ_{tw}) [106-108]. The obtainable MFIS is temperature dependent. In addition to the twinning stress, also the tetragonality of the crystal lattice and the magnetocrystalline anisotropy are strongly temperature dependent [59,94,96-98,106]. The lattice parameter *a* in the **5M** martensite increases slightly and the parameter *c* decreases with the decreasing temperature resulting in the increase of the lattice distortion while cooling down [94,96]. Heczko *et al.* [97,98,106] have shown that the magnetocrystalline anisotropy increases with decreasing temperature saturating at low temperatures. In [97] the MFIS of the alloy $Ni_{49.7}Mn_{29.1}Ga_{21.2}$, increases with the decreasing temperature.

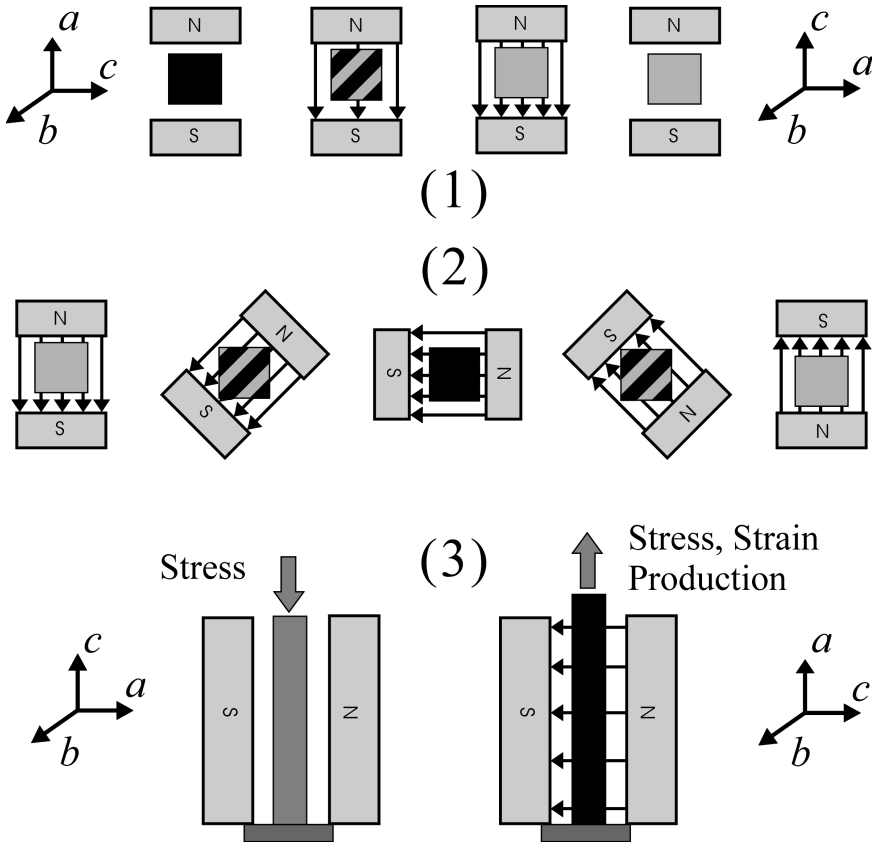

Figure 2. MSM element (1) in the constant unidirectional and (2) in the rotating magnetic field and (3) in the actuator. *a*, *b* and *c* are crystallographic axes of martensite (*c* < *a*,*b*). The short *c*-axis is the easy axis of magnetization. *Publication VIII.*
[Reprinted from The Encyclopedia of Materials: Science and Technology Vol. **1** *O. Söderberg, A. Sozinov and V.K. Lindroos* **Giant magnetostrictive materials.** In: J. Buschow (Ed.), p. 1. Copyright (2004), with permission from Elsevier.]

In Figure 2, magnetic shape memory is illustrated with the Ni-Mn-Ga alloy having a modulated structure. The crystallographic *c*-axis is the shortest one and the easy axis of magnetization. The magnetic anisotropy is large compared to the energy needed for the twin-boundary motion. The preferred direction of magnetization changes across the twin boundary. Consequently, the applied magnetic field creates a difference in magnetic energy across the twin boundary. This energy exerts pressure on the twin boundary to grow those twin variants that are favourably oriented to the direction of magnetization (Figure 2-1). Those martensite variants having the *c*-axis along the magnetic field become dominant and the material contracts in the direction of the applied field.

This shape change, MFIS, remains even after removing the magnetic field. Actuation is possible only either by turning the magnetic field perpendicular to its original orientation, for example, by rotation (Figure 2-2) or with an external spring-back load (Figure 2-3). Then, the single-variant structure obtained at the beginning changes to another single-variant structure generating the actuation of MFIS.

4.1. Magneto-mechanical stress requirement for MSME

Several model approaches have been proposed to help understand the magneto-mechanical phenomena observed in the ferromagnetic shape memory alloys [15,106-113]. Likhachev presented in [15,108] the magneto-mechanical model for the possibility of MSME. This approach is applied to the selected Ni-Mn-Ga alloys in the present thesis. According to this, the alloy can be transformed between two single twin variants with twin-boundary motion, if the magnetic-field-induced stress (σ_{mag}) exceeds the twinning stress (σ_{tw}). Since the σ_{mag} cannot exceed the saturation value given by the ratio of the magnetic anisotropy (K_U) and the maximum field-induced strain from Eq. (3), this requirement can be formulated

$$\sigma_{mag} = \frac{K_U}{\varepsilon_0} > \sigma_{tw} \qquad (4)$$

The value for the strain ε_0 can also be evaluated from the experimental stress-strain curve as the maximum strain of the detwinning. The maximum magnetic-field-induced stresses, together with the twinning stress and the observed MFIS of some Ni-Mn-Ga alloys, are presented in Table 1. These results coincide with Eq. (4) rather well.

Table 1. The maximum magnetic-field-induced stresses together with the twinning stresses and the observed MFIS values for some Ni-Mn-Ga alloys.

Alloy (martensite crystal structure)	$\lvert K_U \rvert$ (10^5 x J/m^3)	ε_0 (%)	σ_{mag} (MPa)	σ_{tw} (MPa)	Observed MFIS (%)	Reference
$Ni_{48}Mn_{30}Ga_{22}$ (**5M**)	1.3	5.8	2.25	2.12	5	[108]
$Ni_{49.2}Mn_{29.6}Ga_{21.2}$ (**5M**)	1.22	5.7	2.14	2	4.78	[57]
	1.45	5.8	2.1	1	5.8	[58]
$Ni_{50.7}Mn_{28.4}Ga_{20.9}$ (**5M**)	1.67	6.2	2.8	1-4	> 6	[56]
$Ni_{48.8}Mn_{29.7}Ga_{21.5}$ (**7M**)	1.6	10.66	1.5	1.5 (< 2)	9.5	[22,114]
	1.6 (*a*) 0.7 (*b*)	10.66	1.9	1.1	9.4	[58]
$Ni_{50.5}Mn_{29.4}Ga_{20.1}$ (**7M**)	1.74 (*a/c*)	10.7	1.6	3-5	0.47	[56]
$Ni_{50.5}Mn_{30.4}Ga_{19.1}$ (**T**)	1.44	21.0	0.7	17-25	None	[56]
$Ni_{52.1}Mn_{27.3}Ga_{20.6}$ (**T**)	2.03	20.5	1.1	15	< $2x10^{-2}$	[57,58]

5. EXPERIMENTAL METHODS

The microstructures and the properties of the alloys were studied by several experimental methods in the research leading to this thesis. The X-ray method for crystallographic studies is presented in *Publication I*, the differential scanning calorimetry (DSC), *ac* magnetic susceptibility and optical methods in *Publication II*, the mechanical and magneto-mechanical testing in *Publications III-IV* and *VI-VII*. More detailed information about the applied methods is given by Lanska and Ullakko [100], Seuranen [115], Koho [53] and Jääskeläinen [116]. The measurement of the internal friction in *Publication V* was carried out by means of the the automated inverted pendulum equipment presented in *Attachment 1*. The chemical analysis was carried either by energy dispersive spectrometry (EDS) or wavelength dispersive spectrometry (WDS) or both after the heat treatment procedure for the homogenized alloy and later on by EDS-method for the ready specimens. Details and limitations of the applied chemical analysis methods are discussed in [117].

6. CRYSTAL STRUCTURES OF THE STUDIED ALLOYS AT AMBIENT TEMPERATURE

Altogether, 37 Ni-Mn-Ga alloys are studied in the *Publications*. Of these, 33 alloys are from *Publication I* and four alloys from *Publications IV, V* and *VII*. The alloys are presented in Table 2 together with their chemical compositions, the parent-martensite (**P**↔**M**) transformation temperatures together with the Curie points, the valence electron concentrations as well as the crystal structures at ambient temperature. Here, the alloys with the multiple-step (**P**→**M**→**IM**) and single-step (**P**→**M**) structural transformations are not separated from each other and no separation of the alloys showing the hysteresis in magnetic transition is made.

Table 2 shows several previously unpublished alloy compositions with ferromagnetic modulated martensitic crystal structure (**5M** or **7M**) at ambient temperature. The martensitic transformation region of these alloys yields up to 353 K and they are good candidates for the practical applications of MSM. According to Table 2, it is clear that the martensitic alloys with $T_M = (M_s+M_f)/2 > T_C$ have the non-modulated tetragonal crystal structure. The **5M** and the **7M** structures were observed only in the alloys $T_M < T_C$. In Figure 3, the alloys of *Publication I* are plotted according to their *c/a* ratio as a function of the martensitic transformation temperature and as a function of the valence electron concentration *e/a*. At ambient temperature, the alloys with the **T** martensite have a *c/a* ratio close to 1.2, while the **5M** alloys show the *c/a* ratio in the area 0.9-0.95 and the **7M** alloys approximately 0.89. The **5M** alloys exist until *e/a* close to 7.70 and the **T** alloys mainly above *e/a* >7.68, while the **7M** alloys stay within the range of $7.67 < e/a \leq 7.71$.

It is important to know how the chemical composition influences the crystal parameters, since they determine the crystal type and affect the obtainable stress-induced and magnetic-field-induced strains of the alloy. In *Publication I,* the evolution of lattice parameters for the **5M** and **T** alloys is plotted as a function of their transformation temperatures (Figure 4). There is no chart for the **7M** alloys, since the *c/a* ratio of all the studied alloys was approximately the same, i.e. 0.890-0.894. Their T_M values were also in the rather narrow temperature range of 335-353 K. According to these results, the theoretical maximum strain values from Eq. (3) are approximately 7 % for the **5M** martensite, 11 % for the **7M** martensite and 23 % for the **T** martensite.

Table 2.
The chemical compositions of the studied alloys with the parent-martensite transformation temperatures, the average of Curie points during heating and cooling, the valence electron concentrations and the type of the martensitic phase at 298 K.

Alloy	Content (at %)			M_s	M_f	A_s	A_f	T_C	*e/a*	Phase
	Ni	Mn	Ga	(K)	(K)	(K)	(K)	(K)		
1	50.7	28.4	20.9	334	325	339	345	367	7.685	**5M**
2	50.7	28.3	21.0	330	323	338	343	363	7.681	**5M**
3	50.7	27.8	21.5	325	323	331	334	371	7.661	**5M**
4	50.6	28.5	20.9	333	331	339	341	371	7.682	**5M**
5	50.0	29.8	20.2	344	340	347	351	370	7.692	**5M**
6	50.0	28.9	21.1	321	311	320	330	374	7.656	**5M**
7*	49.2	29.6	21.2	297	293	302	306	372	7.628	**5M**
8	49.9	29.9	20.2	344	338	350	354	369	7.690	**5M**
9	49.7	29.1	21.2	311	309	319	321	372	7.643	**5M**
10	49.6	29.2	21.2	303	301	309	309	376	7.640	**5M**
11	49.2	30.6	20.2	328	323	333	337	370	7.668	**5M**
12	49.1	30.7	20.2	324	321	332	335	370	7.665	**5M**
13	49.0	30.3	20.7	312	309	318	323	370	7.642	**5M**
14	48.5	30.3	21.2	302	299	305	308	372	7.607	**5M**
15	51.0	28.5	20.5	356	350	354	360	365	7.710	**7M**
16	50.5	29.4	20.1	351	343	348	357	366	7.711	**7M**
17	49.5	30.3	20.2	341	337	344	348	363	7.677	**7M**
18	48.8	31.4	19.8	337	333	338	342	368	7.672	**7M**
19*	48.8	29.7	21.5	337	333	338	342	368	7.604	**7M**
20	54.9	23.8	21.3	559	541	568	587	360	7.795	**T**
21	54.0	24.7	21.3	497	487	498	510	328	7.768	**T**
22	53.9	24.4	21.7	530	524	551	560	336	7.749	**T**
23	53.7	26.4	19.9	523	512	538	546	344	7.815	**T**
24	53.3	24.6	22.1	465	459	468	476	371	7.715	**T**
25	52.9	25.0	22.1	348	344	354	363	356	7.703	**T**
26	52.8	25.7	21.5	390	367	377	404	382	7.724	**T**
27	52.7	26.0	21.3	434	416	424	446	376	7.729	**T**
28	52.4	25.6	22.0	423	414	424	434	375	7.692	**T**
29	52.3	27.4	20.3	398	391	403	408	380	7.757	**T**
30	51.7	27.7	20.6	383	369	381	394	386	7.726	**T**
31	51.5	26.8	21.7	393	374	380	400	377	7.677	**T**
32	51.2	27.4	21.4	371	366	371	375	370	7.680	**T**
33	51.0	28.7	20.3	379	366	376	385	372	7.721	**T**
34	50.5	30.4	19.1	391	376	383	397	378	7.751	**T**
35	47.0	33.1	19.9	326	323	329	331	366	7.614	**T**
36*	54.5	21.5	24.0	373	365	376	384	371	7.675	**T**
37*	52.1	27.3	20.6	399	391	401	410	380	7.736	**T**

* From *Publications IV, V* and *VII.*

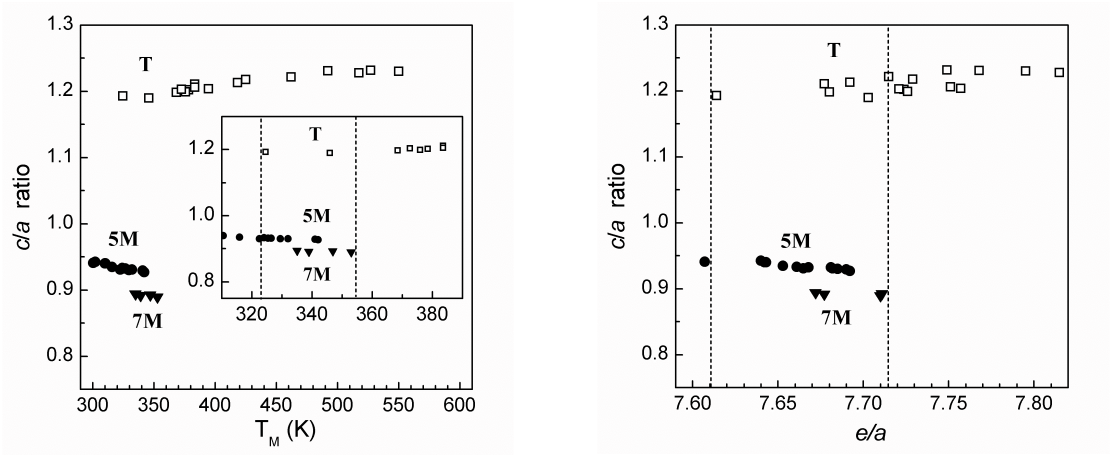

Figure 3. The *c/a* ratio of the alloys with the **5M**, the **7M** and the **T** structure at T = 298 K as a function of (a) martensitic transformation average temperature (T_M) and (b) the valence electron concentration *e*/*a*. Temperature region with several crystal structures is presented (a) in the insert and (b) with the dotted lines. *Publication I.*
[Reprinted from Journal of Applied Physics Vol. **95** *N. Lanska, O. Söderberg, A. Sozinov, Y. Ge, K. Ullakko, V.K. Lindroos,* **Composition and temperature dependence of the crystal structure in Ni-Mn-Ga alloys**, p. 8077. Copyright (2004), with permission from American Institute of Physics.]

7. TRANSFORMATION SEQUENCES IN SELECTED ALLOYS

As shown before, it is necessary to know certain processing parameters of the alloy to obtain the solid-state transformations in the desired temperature region. Study of the melting and solidification as well as **$L2_1 \rightarrow B2'$** transition is reported in brief in *Publication II* for Alloys 34 and 36. It was confirmed that their melting and solidification took place in a temperature region of 1380-1400 K, while the homogenizing of the alloys should be carried out above 990 K.

The information relating to the transformation sequence of the Ni-Mn-Ga alloys is important for determining the service temperatures of the MSM effect. The information of the temperature regions is needed where the correct twinned martensite **5M** or **7M** structure appears. The magnetic transitions during both heating and cooling should also be established to ensure that the desired structure is ferromagnetic. In *Publication II*, the transformation paths of Alloys 34 and 36 were examined in detail, whereas in *Publication III*, a more general approach was presented, dealing with the transformation sequence of Alloys 18, 29 and 35.

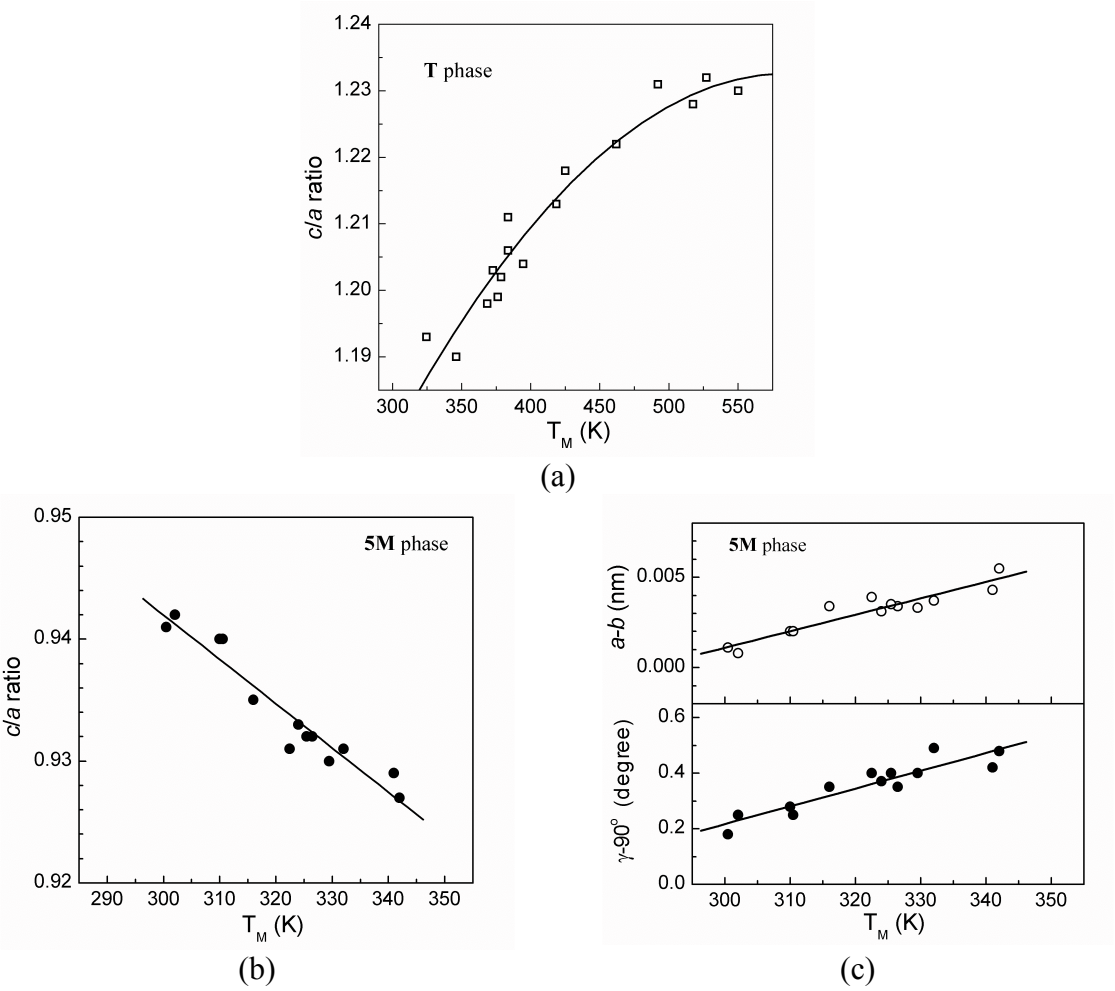

Figure 4. *c/a* ratio at T=298 K as a function of the martensitic transformation average temperature T_M (a) for the alloys with **T** phase and (b) for the alloys with **5M** phase. (c) Monoclinic distortion for the alloys with **5M** phase at T=298 K as a function of the martensitic transformation average temperature T_M; difference of parameters *a* and *b*, (*a*-*b*) and deviation of the angle γ from 90°, (γ-90). *Publication I*.

[Reprinted from Journal of Applied Physics Vol. **95** *N. Lanska, O. Söderberg, A. Sozinov, Y. Ge, K. Ullakko, V.K. Lindroos,* **Composition and temperature dependence of the crystal structure in Ni-Mn-Ga alloys**, p. 8076. Copyright (2004), with permission from American Institute of Physics.]

In Figure 5, three different paths of transformations are presented. In cooling Alloy 35, the paramagnetic parent phase turns at first ferromagnetic, and, at lower temperature, the structural transition occurs in one step to the ferromagnetic **T** martensite: $\mathbf{P_{param}}\rightarrow\mathbf{P_{ferrom}}\rightarrow\mathbf{T_{ferrom}}$ (Figure 5a). Alloy 29 shows, at first, the structural transition as the paramagnetic parent phase transforms to the paramagnetic **T** martensite and, in further cooling, the martensite phase becomes ferromagnetic: $\mathbf{P_{param}}\rightarrow\mathbf{T_{param}}\rightarrow\mathbf{T_{ferrom}}$ (Figure 5b). In this case, the structural transformation is detected only in the DSC measurement, since it occurs above the Curie point and is not, therefore, detectable in the *ac* magnetic susceptibility curve. In Alloy 18, the parent phase has, at first, the magnetic transition and the first martensite to appear is the **7M** structure. Clearly, below this transformation, an intermartensitic transformation to the **T** martensite takes place leading to the total transformation sequence of $\mathbf{P_{param}}\rightarrow\mathbf{P_{ferrom}}\rightarrow\mathbf{7M_{ferrom}}\rightarrow\mathbf{T_{ferrom}}$ (Figure 5c). In heating, the transformation sequence is the opposite of certain temperature deviations of the structural transitions. The Curie points during heating and cooling were the same for Alloys 35 and 18 (Figures 5a and 5c), while, in Alloy 29 (Figure 5b), the magnetic transition had a clear hysteresis. The Curie point in cooling (T_{Cc}) was about 10 K below that measured during heating (T_{Ch}). The hysteresis of the magnetic transition is also observed with Alloy 36 in *Publication V* and with Alloy 26 in *Publication VI* (Figure 6).

Both of these alloys also showed the co-occurrence of the structural and magnetic transitions. The transformation sequences of Alloy 26 were $\mathbf{P_{param}}\rightarrow\mathbf{P_{ferrom}}\rightarrow\mathbf{T_{ferrom}}$ during cooling and $\mathbf{T_{ferrom}}\rightarrow\mathbf{T_{param}}\rightarrow\mathbf{P_{param}}$ during heating (Figure 6a). The hysteresis with $T_{Ch} > T_{Cc}$ is in accordance with the suggestion of the different Curie points of the cubic parent phase ($T_{C\mathbf{P}}$) and the tetragonal martensitic phase ($T_{C\mathbf{M}}$) [52,105]. In Alloy 34 in *Publication II*, the magnetic hysteresis was encountered with a double-step structural transformation (Figure 6b). Here, the magnetic transition during cooling occurred in the **7M** structure ($\mathbf{P_{param}}\rightarrow\mathbf{7M_{param}}\rightarrow\mathbf{7M_{ferrom}}\rightarrow\mathbf{T_{ferrom}}$) and when the material was heated, it took place in the **T** martensite ($\mathbf{T_{ferrom}}\rightarrow\mathbf{T_{param}}\rightarrow\mathbf{7M_{param}}\rightarrow\mathbf{P_{param}}$). Consequently, the hysteresis in magnetic transition is suggested to be due to the different Curie points of the different martensitic phases. The magnetic transition in the **7M** martensite occurs at lower temperature than in the **T** martensite, i.e. $T_{C\mathbf{7M}} < T_{C\mathbf{T}}$. To confirm this suggestion, the alloy was cooled between the martensitic and intermartensitic transformation temperatures in such a way that the structure was the **7M**. Thereafter, the material was heated to the parent phase. The Curie point did not show the hysteresis in this measurement, since the magnetic transition took place in the **7M** structure during both cooling and heating.

Figure 7 shows the Curie points together with the valence electron concentration *e/a* as a function of the *c/a* ratio. The Curie points of the $T_{C\mathbf{T}}$ decrease from 386 K to 328 K, while the *c/a* at ambient temperature increases from 1.2 to 1.235. The $T_{C\mathbf{7M}}$ decreases much less and the average of the measured Curie points is 372 K. The Curie point of the cubic parent phase ($T_{C\mathbf{P}}$) is approximately 366 K. The high $T_{C\mathbf{P}}$ value 378 K of Alloy 26 is a combination of the different Curie points weighted by the phase quantities. This measured value also partly includes the Curie point of the martensitic phase. The obtained results agree well with the suggestions that each phase has its own Curie point and that the Curie point decreases with the increasing lattice volume.

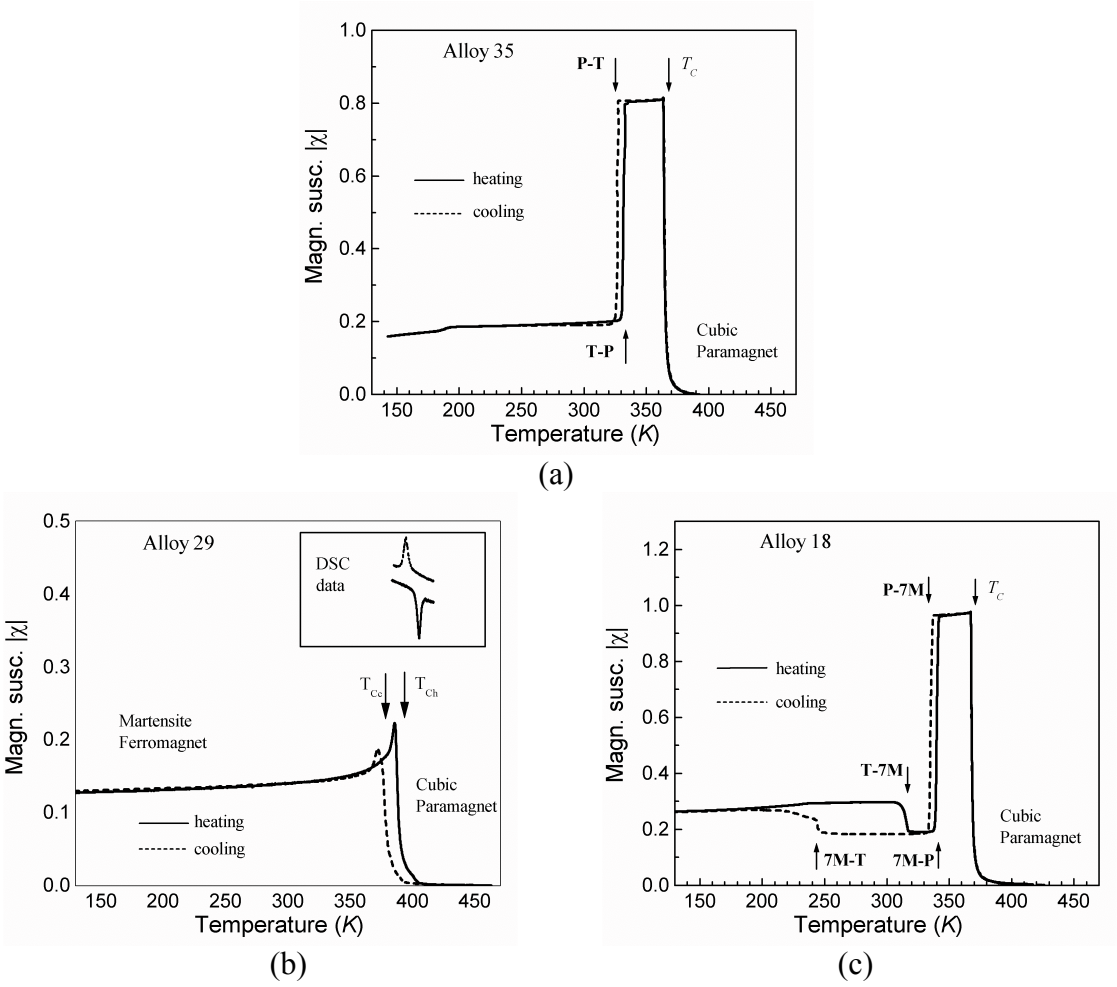

Figure 5. Temperature dependence of the low-field *ac* magnetic susceptibility measured during cooling (dashed) and heating (solid) for (a) Alloy 35, (b) Alloy 29 with DSC data as inset, and for (c) Alloy 18. Arrows mark the phase transformations. **P** – the cubic parent phase, **7M** – the orthorhombic seven-layered martensite phase, **T** – the tetragonal non-modulated martensite phase, T_C – the Curie point, T_{Cc} – the Curie point during cooling, T_{Ch} – the Curie point during heating. *Publications III, VII*.

[Reprinted from Journal de Physique IV Vol. **115** *A. Sozinov, A.A. Likhachev, N. Lanska, O. Söderberg, K. Koho, K. Ullakko, V.K. Lindroos,* **Stress-induced variant rearrangement in Ni-Mn-Ga single crystals with nonlayered tetragonal martensitic structure**, p. 123. Copyright (2004), with permission from EDP Sciences.

Reprinted from Proceedings of SPIE International Society for Optical Engineering Vol. **5053** *A. Sozinov, A.A. Likhachev, N. Lanska, O. Söderberg, K. Ullakko and V.K. Lindroos,* **Effect of crystal structure on magnetic-field-induced strain in Ni-Mn-Ga**, p. 590. Copyright (2003), with permission from SPIE International Society for Optical Engineering.]

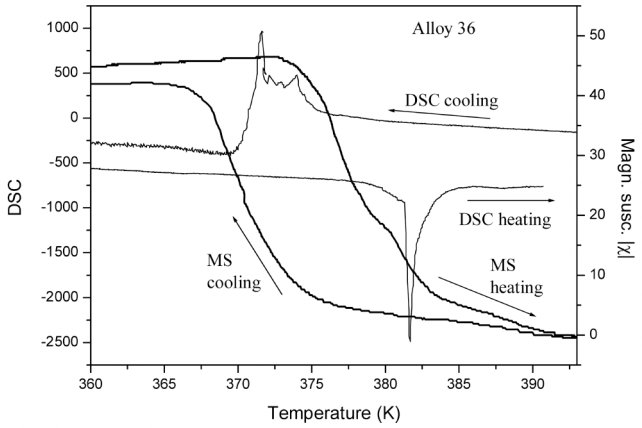

(a)

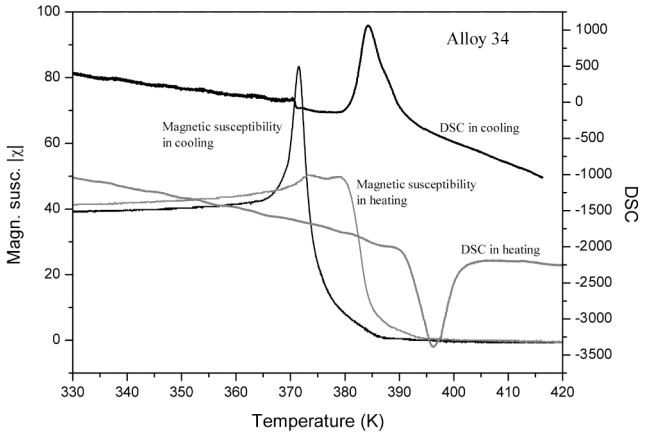

(b)

Figure 6. The *ac* magnetic susceptibility results and the Linkam DSC results for (a) Alloy 36 and (b) Alloy 34. *Publications II, V*.

[Reprinted from Scripta Materialia Vol. **49** *V.G. Gavriljuk, O. Söderberg, V.V. Bliznuk, N.I. Glavatska and V.K. Lindroos*, **Martensitic Transformations and Mobility of Twin Boundaries in Ni_2MnGa Alloys Studied by Using Internal Friction**, p. 805. Copyright (2003), with permission from Elsevier.
Reprinted from Zeitschrift für Metallkunde Vol. **95** *O. Söderberg, M. Friman, A. Sozinov, N. Lanska, Y. Ge, M. Hämäläinen and V.K. Lindroos***, Transformation behaviour of two Ni-Mn-Ga alloys**, p. 728. Copyright (2004), with permission from Carl Hanser Verlag.]

Table 3 shows the alloys with the **7M** or the **T** structure at ambient temperature from Table 2. Now, the structural and magnetic transitions are described in more detail by reporting the transformation temperatures connected to the martensitic and intermartensitic reactions as well as the Curie points during cooling and heating. The Curie point of Table 2 is applied if there is no remarkable hysteresis of the magnetic transition. The transformation sequences are assumed to be as those described above, i.e. the structural phase transformation obeys either **P↔T** or **P↔7M↔T** transformation path and the crystal structure at the Curie point is given according to the phase existing at the magnetic transition.

In those alloys in Table 3 showing the magnetic transition in a single-phase region, the Curie point is either the one of the parent phase (T_{CP}) or the one of the **T** martensite (T_{CT}). In Alloys 25, 31 and 33, no hysteresis exists at the Curie point, even though the magnetic transition occurs in addition to the single-phase region in a two-phase structure. It is suggested that in these alloys the observed Curie point has been connected to the single phase. This gives the following Curie points: T_{CP} in Alloy 25, T_{CT} in Alloy 31 and T_{C7M} in Alloy 33. With Alloys 26, 34 and 36 showing the hysteresis of the magnetic transition, the suggestions $T_{CP} < T_{CM}$ and $T_{C7M} < T_{CT}$ are applied. Consequently, the Curie points during cooling are T_{CP} in Alloy 26, T_{C7M} in Alloy 34 and T_{CT} in Alloy 36. In heating they are T_{CT}, T_{CT} and T_{CT}, respectively. For Alloy 32, the low value of the Curie point is assumed to be T_{CP}. Alloy 30 with two double-phase transitions shows during cooling the T_{C7M}, while, in heating, the high Curie point is supposed to be T_{CT}.

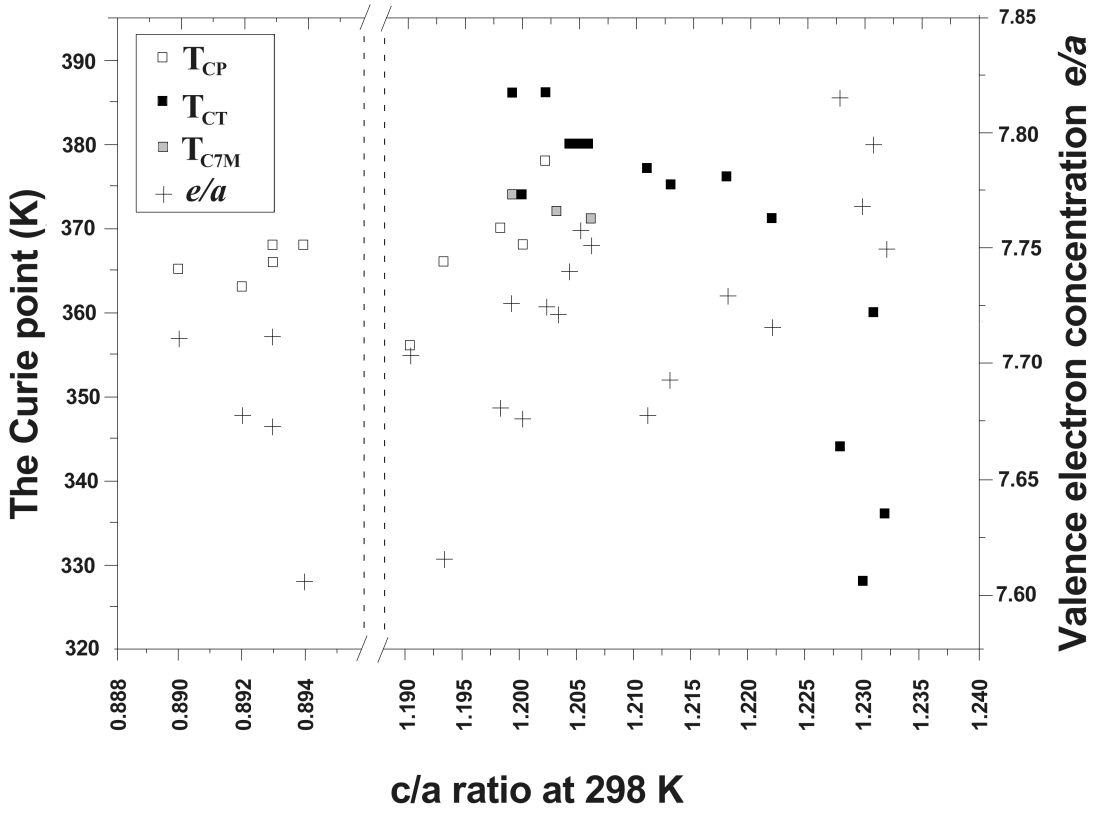

Figure 7. The Curie points connected to different structural phases and the valence electron concentrations of the alloys given in Table 3 as function of the *c/a* ratios.

Table 3. The structural and magnetic transitions of the alloys showing the **7M** or **T** structure at ambient temperature. The previously unpublished data data was obtained during the HUT-MSM project.

M_s, M_f = the start and the finish temperatures of **P→M** (**T** or **7M**) transformation. $M_{s7M\rightarrow T}$, $M_{f7M\rightarrow T}$ = the start and the finish temperatures of the intermartensitic transformation **7M→T**. A_s, A_f = the start and the finish temperatures of the reverse transformation **M** (**T** or **7M**) → **P**. $A_{sT\rightarrow 7M}$, $A_{fT\rightarrow 7M}$ = the start and the finish temperatures of the intermartensitic reverse transformation **T→7M**. T_{Cc} = the Curie point during cooling. T_{Ch} = the Curie point during heating. The crystal structure during the magnetic transition is given below the Curie point as well as below certain *c/a* ratios. *Publications* are marked *PI, PII, PIII, PIV, PV, PVI* and *PVII*.

Alloy	Composition	*e/a*	*c/a* *at 298K*	*c/a* *at other temp.*	M_s (K)	M_f (K)	M_{s7M-T} (K)	M_{f7M-T} (K)	A_s (K)	A_f (K)	A_{sT-7M} (K)	A_{fT-7M} (K)	T_{Cc} (K)	T_{Ch} (K)
15	$Ni_{51.0}Mn_{28.5}Ga_{20.5}$	7.710	0.890		356	350	233	223*[1]	354	360	314*[1]	325*[1]	365	
PI, PIV													**P**	
16	$Ni_{50.5}Mn_{29.4}Ga_{20.1}$	7.711	0.893		351	343	238	228	348	357	not obs.	313	366	
PI, PIV														
[99]													**P**	
17	$Ni_{49.5}Mn_{30.3}Ga_{20.2}$	7.677	0.892		341	337	283	273*[1]	344	348	337*[1]	343	363	
PI, PIV													**P**	
18	$Ni_{48.8}Mn_{31.4}Ga_{19.8}$	7.672	0.893		337	333	245	225*[1]	338	342	306	316	368	
PI, PIII			**7M**										**P**	
			1.187											
			T*[2]											
19	$Ni_{48.8}Mn_{29.7}Ga_{21.5}$	7.604	0.894		337	333	245		338	342	306	316	368	
PIV, PVII														
[22]													**P**	
20	$Ni_{54.9}Mn_{23.8}Ga_{21.3}$	7.795	1.231		559	541			568	587			360	
PI													**T**	
21	$Ni_{54.0}Mn_{24.7}Ga_{21.3}$	7.768	1.230		497	487			498	510			328	
PI													**T**	
22	$Ni_{53.9}Mn_{24.4}Ga_{21.7}$	7.749	1.232		530	524			551	560			336	
PI													**T**	
23	$Ni_{53.7}Mn_{26.4}Ga_{19.9}$	7.815	1.228		523	512			538	546			344	
PI, PII													**T**	
24	$Ni_{53.3}Mn_{24.6}Ga_{22.1}$	7.715	1.222		465	459			468	476			371	
PI													**T**	
25	$Ni_{52.9}Mn_{25.0}Ga_{22.1}$	7.703	1.190		348	344			354	363			356	
PI													**P**	**T+P**
26	$Ni_{52.8}Mn_{25.7}Ga_{21.5}$	7.724	1.202		390	367			377	404			378	386
PI, PVI													**P+T**	
27	$Ni_{52.7}Mn_{26.0}Ga_{21.3}$	7.729	1.218		434	416			424	446			376	
PI, PVII													**T**	
28	$Ni_{52.4}Mn_{25.6}Ga_{22.0}$	7.692	1.213		423	414			424	434			375	
PI													**T**	
29	$Ni_{52.3}Mn_{27.4}Ga_{20.3}$	7.757	1.205		398	391			403	408			380	
PI, PIII													**T**	
30	$Ni_{51.7}Mn_{27.7}Ga_{20.6}$	7.726	1.199		383	369	368	357	381	394	not obs.	not obs.	374	386
PI													**P+7M**	**T+P**
31	$Ni_{51.5}Mn_{26.8}Ga_{21.7}$	7.677	1.211		393	374			380	400			377	
PI													**P+T**	**T**
32	$Ni_{51.2}Mn_{27.4}Ga_{21.4}$	7.680	1.198		371	366			371	375			370	
PI													**P**	**T**
33	$Ni_{51.0}Mn_{28.7}Ga_{20.3}$	7.721	1.203		379	366	343	324	376	385	188	190	372	
PI													**P+7M**	**7M**
34	$Ni_{50.5}Mn_{30.4}Ga_{19.1}$	7.751	1.206	0.884	391	376	331	311	383	397	379		371	380
PI, PII			**T**	**7M**									**7M**	**T+7M**
[56,99]				350K										
35	$Ni_{47.0}Mn_{33.1}Ga_{19.9}$	7.614	1.193		326	323			329	331			366	
PI, PIII													**P**	
36	$Ni_{54.5}Mn_{21.5}Ga_{24.0}$	7.675	1.200		373	365			376	384			368	374
PV													**P+T**	**T**
37	$Ni_{52.1}Mn_{27.3}Ga_{20.6}$	7.739	1.204		399	391			401	410			380	
PV, PVII													**T**	
[57,58]														

*[1] DSC results from 2 K/min measurements – in *Publication IV,* only magnetic susceptibility results are taken into account. *[2]The **7M** value corresponds to the structure during cooling at ambient temperature and **T** the structure after cooling to 80 K and heating to ambient temperature.

A 7M ambient

- $T_{Cc}=T_{Ch}=T_C=T_{CP}$
- $M_s,M_f,A_s,A_f < T_C$
- $M_{s7M\rightarrow T}$, $A_{sT\rightarrow 7M} < T_{ambient}$

Cooling	T_{ferrom}	$7M_{ferrom}$	P_{ferrom}	P_{param}
Temp.	$M_{s7M\rightarrow T}$ $A_{fT\rightarrow 7M}$	*Ambient* M_f A_s		T_{CP}
Heating	T_{ferro}	$7M_{ferrom}$	P_{ferrom}	P_{param}

- At ambient temperature the **7M** structure
- In cooling the ferromagnetic **7M** at $M_f > T > M_{s7M\rightarrow T}$
- In heating ferromagnetic **7M** at $A_{fT\rightarrow 7M} < T < A_s$
- Alloys *15, 16, 17, 18,19*

B 7M above

- $T_{Cc}=T_{Ch}=T_C=T_{C7M}$
- $M_s > T_C > M_f$, $T_C < A_s,A_f$
- $M_{s7M\rightarrow T}$, $M_{f7M\rightarrow T} > T_{ambient}$
- $T_{ambient} > A_{sT\rightarrow 7M}$, $A_{fT\rightarrow 7M}$

Cooling	T_{ferrom}	$7M_{ferrom}$	$7M_{param}$	P_{param}
Temp.	*Ambient* $M_{s7M\rightarrow T}$		T_C	M_f
	$A_{f7M\rightarrow T}$		A_s	
Heating	T_{ferrom}	$7M_{ferrom}$	$7M_{param}$	P_{param}

- At ambient temperature during cooling the **T** structure and during heating the **7M** structure
- In cooling the ferromagnetic **7M** at $M_f > T > M_{s7M\rightarrow T}$
- In heating ferromagnetic **7M** at $A_{fT\rightarrow 7M} < T < T_C$
- Alloy 33

C 7M co-transition

- $T_{Cc}=T_{C7M} \neq T_{Ch}=T_{CT}$
- $T_{Cc} < M_s$, M_f
- $T_{ambient} < M_{s7M\rightarrow T}$, $M_{f7M\rightarrow T}$
- $T_{Ch} \leq A_{sT\rightarrow 7M}$, $A_{fT\rightarrow 7M}$, A_s, A_f

Cooling	T_{ferrom}	$7M_{ferrom}$	$7M_{param}$	P_{param}
Temp.	*Ambient* $M_{s7M\rightarrow T}$		T_{Cc} M_f	
			T_{Ch} $A_{sT\rightarrow 7M}$	A_s
Heating	T_{ferrom}		$7M_{param}$	P_{param}

- The ferromagnetic **T** structure at ambient temperature
- In cooling the ferromagnetic **7M** at $T_{Cc} > T > M_{s7M\rightarrow T}$
- In heating the ferromagnetic **7M** at $A_{fT\rightarrow 7M} < T < T_C$
- Alloys *30, 34*

D T high

- $T_{Cc}=T_{Ch}=T_C=T_{CT}$
- $T_C < M_s,M_f,A_s,A_f$

Cooling	T_{ferrom}	T_{param}	P_{param}
Temp.	*Ambient*	T_{CT}	M_f A_s
Heating	T_{ferrom}	T_{param}	P_{param}

- At ambient temperature the **T** structure
- In cooling and heating the ferromagnetic **T** at $T_C > T$
- Alloys *20, 21, 22, 23, 24, 27, 28, 29,37*

E T low

- $T_{Cc}=T_{Ch}=T_C=T_{CP}$
- $M_s,M_f \leq T_C$
- $A_s,A_f < T_C$ or $T_C \approx A_s$

Cooling	T_{ferrom}	P_{param}	P_{param}
Temp.	*Ambient*	M_f A_s	T_{CP}
Heating	T_{ferrom}	P_{param}	P_{param}

- At ambient temperature the **T** or **P** structure
- In cooling the ferromagnetic **T** at $M_f > T$
- In heating the ferromagnetic **T** at $T \leq A_s$
- Alloys 32, 35

F T co-transition

- $T_{Cc}=T_{CP} \neq T_{Ch}=T_{CT}$
- $M_s < T_{Cc} < M_f$
- $A_s < T_{Ch} < A_f$
- $T_{ambient} < M_s,M_f,A_s,A_f$

Cooling	T_{ferrom}	$T_{ferrom}+P_{ferrom}$	$T_{param}+P_{param}$	P_{param}
Temp.		M_f T_{Cc}		M_s
		A_s	T_{Ch} A_f	
Heating	T_{ferrom}	$T_{ferrom}+P_{ferrom}$	$T_{param}+P_{param}$	P_{param}

- The ferromagnetic **T** structure at ambient temperature
- In cooling the ferromagnetic **T** at $M_f > T$
- In heating the ferromagnetic **T** at $T < A_s$
- Alloys *25,26,31,36*

Figure 8. The classification of the alloys in Table 3 into the six groups (***A-F***) according to their structural and magnetic transitions.

The ferromagnetic **7M** or **T** phases of the alloys given in Table 3 can be divided into six groups as shown in Figure 8. This division is carried out by the structural and magnetic transitions. Alloys in the group ***A* 7M ambient** show the **7M** structure at ambient temperatures. In the group ***B* 7M above**, the **7M** phase exists during cooling above ambient temperature and during heating it appears in a rather broad temperature region. Alloys in the group ***C* 7M co-transition** have a temperature region where the **7M** phase exists during cooling, but, during heating, the reverse intermartensitic and reverse reactions are very close to each other and the magnetic transition. The group ***D* T high** shows the **T** phase alloys with the structural transformations clearly above the Curie point. Those alloys having the magnetic transition above the structural one belong to the group ***E* T low**. The group ***F* T co-transition** includes alloys showing co-occurrence of the structural and magnetic transitions. Figure 8 shows also the temperature limits for the existence of that ferromagnetic twinned martensite that transforms directly from the parent phase, since these phases are the most interesting regarding MSME.

8. MECHANICAL BEHAVIOUR OF THE SELECTED ALLOYS

The mechanical behaviour of the Ni-Mn-Ga alloys depends on their crystal structure and the direction of the applied force, the training status of the material, the mobility of the twin boundaries and the external temperature. These factors are discussed in *Publications I, III, IV, V, VI* and *VII*.

The crystal structure of the Ni-Mn-Ga martensite controls the maximum straining of the material via the lattice distortion, Eq. (3). It also affects the twinning stress. According to the lattice distortion, the maximum straining of different martensites can be given as approximately 6 % for the **5M** alloys, 10 % for the **7M** alloys and 20 % for the **T**-structure (Figure 9).

The twinning stress is a critical factor for the possibility of the MSM effect, since it should be smaller than the magnetically induced force, Eq. (4). With the **5M** structure of Ni-Mn-Ga, the twinning stress in a single-variant state can be less than 1 MPa. In the **7M** structure, it can decrease below 2 MPa in the single-variant state that is obtained with pre-straining (Figure 9b). This pre-straining is carried out in the temperature region of $M_{s\mathbf{7M}\rightarrow\mathbf{T}} < T < A_s$, since the structure should be only of the **7M** phase. In compression, the pre-straining is carried out in three steps in two different crystallographic directions. The first compression along to the specimen height to the crystallographic <100> direction produces a 6 % shape change in height. During this deformation, the stress-strain behaviour is rather rough, while the original, thermally formed, multi-variant state transforms to the two-variant state. The second compression is made along the specimen width and the final compression again along the specimen height, after which the two-variant structure has changed to the single-variant state.

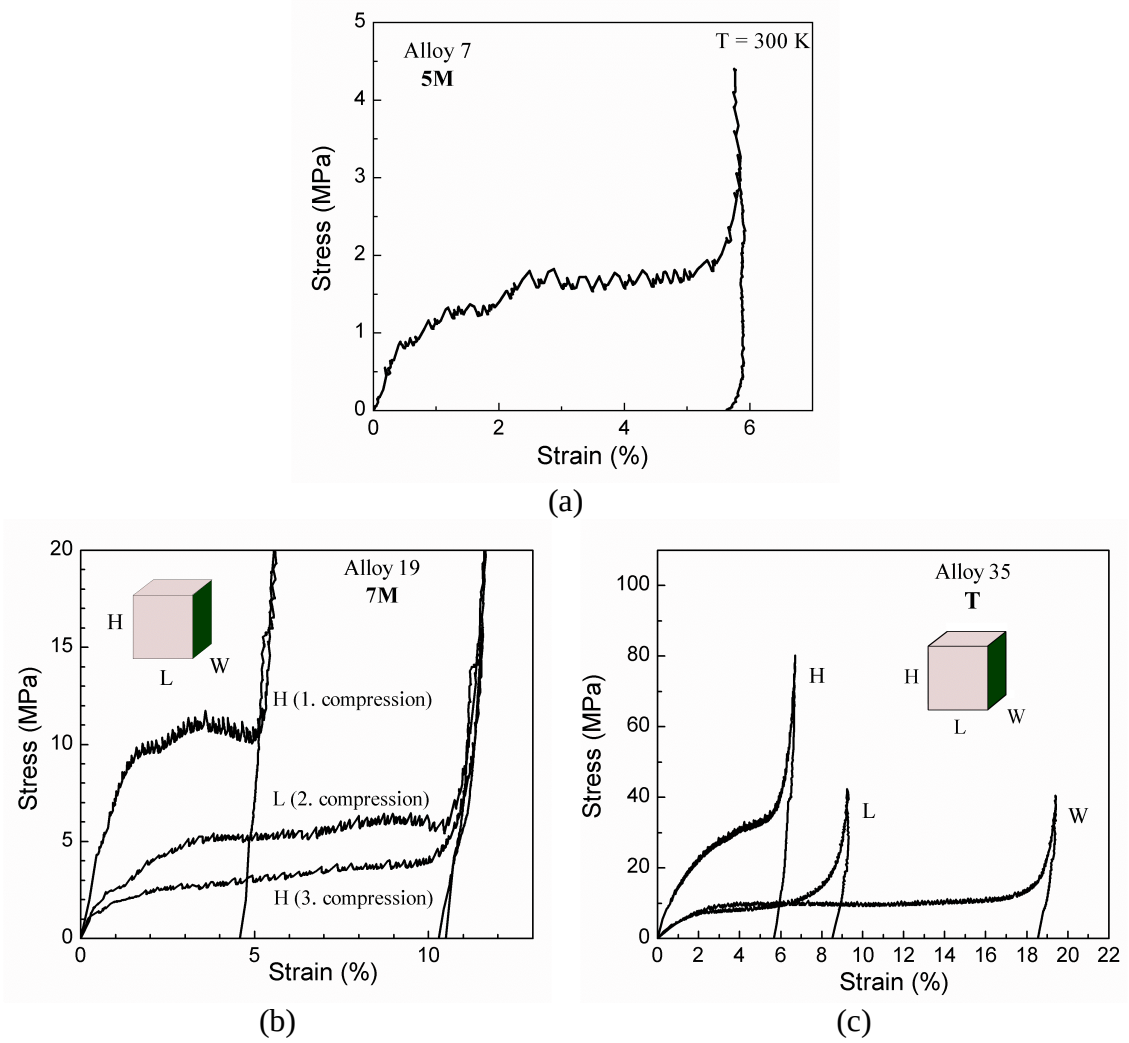

Figure 9. The reorientation of the martensite variants in (a) the **5M** martensite (Alloy 7), (b) the **7M** martensite (Alloy 19) and (c) the non-modulated **T** martensitic (Alloy 35). *Publications III, IV, VII*.

[Reprinted from Proceedings of SPIE International Society for Optical Engineering Vol. **5053** *A. Sozinov, A.A. Likhachev, N. Lanska, O. Söderberg, K. Ullakko and V.K. Lindroos*, **Effect of crystal structure on magnetic-field-induced strain in Ni-Mn-Ga**, p. 588. Copyright (2003), with permission from SPIE International Society for Optical Engineering.

Reprinted from Materials Science and Engineering A Vol. **378/1-2** *A. Sozinov, A.A. Likhachev, N. Lanska, O. Söderberg, K. Ullakko, V.K. Lindroos*, **Stress- and magnetic-field-induced variant rearrangement in Ni-Mn-Ga single crystals with seven-layered martensitic structure**, p. 400. Copyright (2004), with permission from Elsevier.

Reprinted from Journal de Physique IV Vol. **115** *A. Sozinov, A.A. Likhachev, N. Lanska, O. Söderberg, K. Koho, K. Ullakko, V.K. Lindroos*, **Stress-induced variant rearrangement in Ni-Mn-Ga single crystals with nonlayered tetragonal martensitic structure**, p. 125. Copyright (2004), with permission from EDP Sciences.]

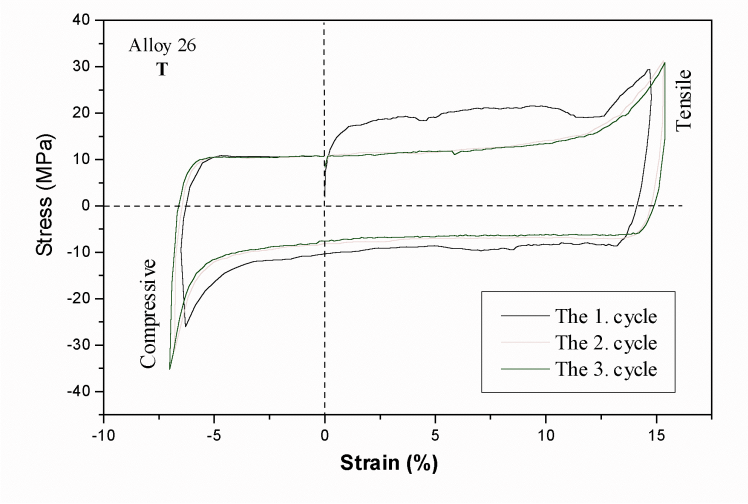

(a)

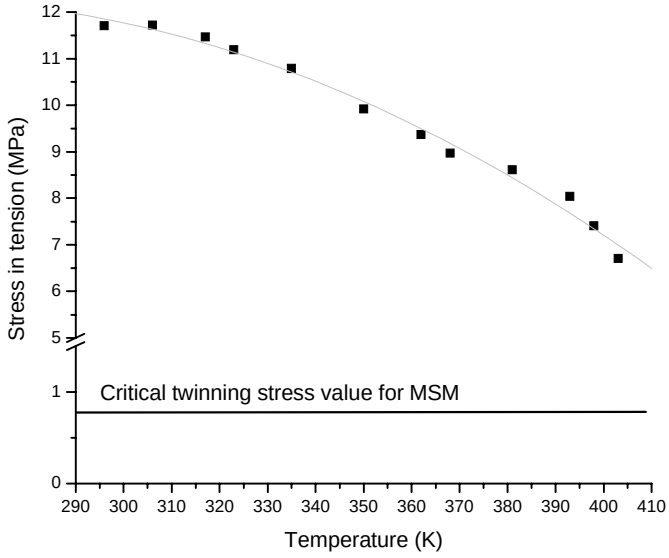

(b)

Figure 10. (a) The complete stress-strain cycles for twin orientation, i.e. detwinning of the non-modulated **T** martensitic structure in Alloy 26. (b) Effect of temperature on the mechanical cycling behaviour shown as a compilation of the stress values at the 4 % straining in tension. *Publication VI.*

[Reprinted from Materials Science and Engineering A Vol. **386** *O. Söderberg, L. Straka, V. Novák, O. Heczko, S.-P. Hannula and V.K. Lindroos,* **Tensile/compression behavior of non-layered tetragonal $Ni_{52.8}Mn_{25.7}Ga_{21.5}$ alloy**, pp. 29,32. Copyright (2004), with permission from Elsevier.]

Obtaining the single-variant state in the non-modulated **T** martensite requires either successive compressions to three different crystallographic directions (Figure 9c) or at least two tensile/compressive deformation cycles (Figure 10a). In compression, the first deformation along the sample height decreases this dimension by 6 %, while the specimen length and width are both increased by 3 %. The structure is transformed to the two-variant state with a variant ratio of about 50/50. The second compression is carried out along the specimen length that is decreased and its width increased by 8-10 %. The height of the specimen is not changed; the only variants affected are in the directions of specimen length and width. In the third compression to the specimen width, the single-variant state is obtained and the sample length is changed by 18-19 %. The twinning stress is set with this method at about 10 MPa (Figure 9c). When the tensile/compressive cycling is applied, the first near to the single-variant state MV1 has been obtained already from the original multi-variant state after the first rough tensile deformation. During the subsequent compression, this variant changes to another single-variant state MV2. Forces needed for this are lower than those during the first tensile section. During the subsequent cycle, the single-variant state MV1 is obtained again in tension and it transforms in compression to the MV2. Now the behaviour of the material has stabilized and the twinning stress on the tensile side is approximately 10 MPa, while in the compressive side only about 6 MPa is needed for twin-variant rearrangement.

The change of the twin structure in the pre-straining with the tensile/compressive cycling is shown in Figure 11. In the thermally formed **T** martensite, the larger twin areas are separated from each other by rather profound borders and the internal twins are narrow with an average width of 2.58 μm (Figure 11a). In the single-variant state, the broad twin boundaries have disappeared and are seen only as faint shadow lines in Figure 11b. The average width of the internal twins has increased to 3.38 μm, while the internal twins are now continuing through the structure. These changes ease the shape change of the material and lead to the decrease of the twinning stress.

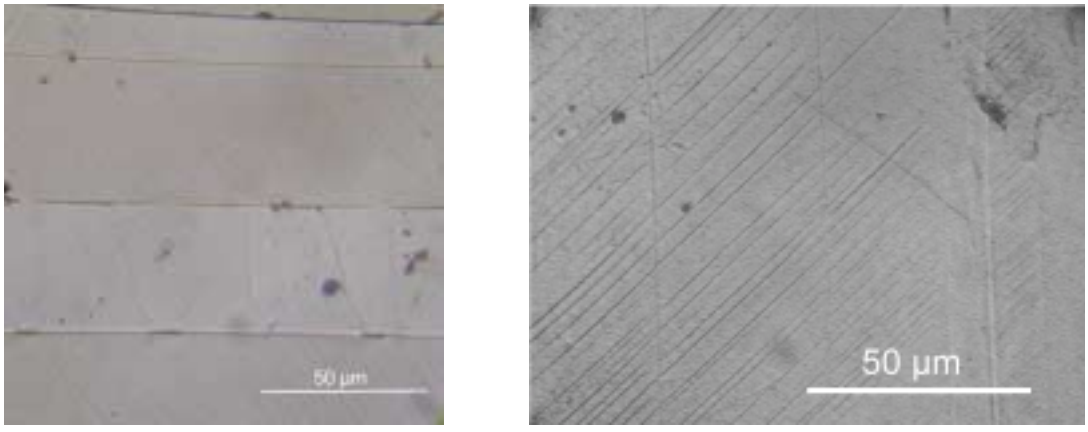

(a) (b)

Figure 11. The morphological structure of a non-modulated tetragonal **T** structure (Alloy 26) at ambient temperature (a) thermally formed in annealed state and (b) after tensile/compression cycling. *Publication VI.*

[Reprinted from Materials Science and Engineering A Vol. **386** *O. Söderberg, L. Straka, V. Novák, O. Heczko, S.-P. Hannula and V.K. Lindroos,* **Tensile/compression behavior of non-layered tetragonal $Ni_{52.8}Mn_{25.7}Ga_{21.5}$ alloy**, p. 28. Copyright (2004), with permission from Elsevier.]

The twinning stress is dependent on the mobility of the twin boundaries that can be studied with the internal friction (IF), the free decay of the enforced vibrations. Césari *et al.* [118] and Seguí *et al.* [119] suggested that the high IF value of the Ni-Mn-Ga modulated martensites is connected to the mobile martensite invariant boundaries and the low elastic modulus. In *Publication V*, the internal friction was studied with the non-modulated **T** Alloys 36 and 37. By measuring the strain-dependent internal friction at different temperatures, the activation enthalpy for the movement of twin boundaries was established as 0.02-0.025 eV in Alloy 36 and 0.03-0.04 eV in Alloy 37. The IF measurements of Alloy 37 are presented in Figure 12.

Both the increase of the IF value and the steeper slope of the IF-strain-curve with the increasing temperature reveal the better mobility of the twin boundaries at high temperatures. This is in accordance with the lower twinning stress values observed at higher temperatures [for example, 59,106] and with the results shown in *Publications III, IV, VI* and *VII* (Figures 10b and 13).

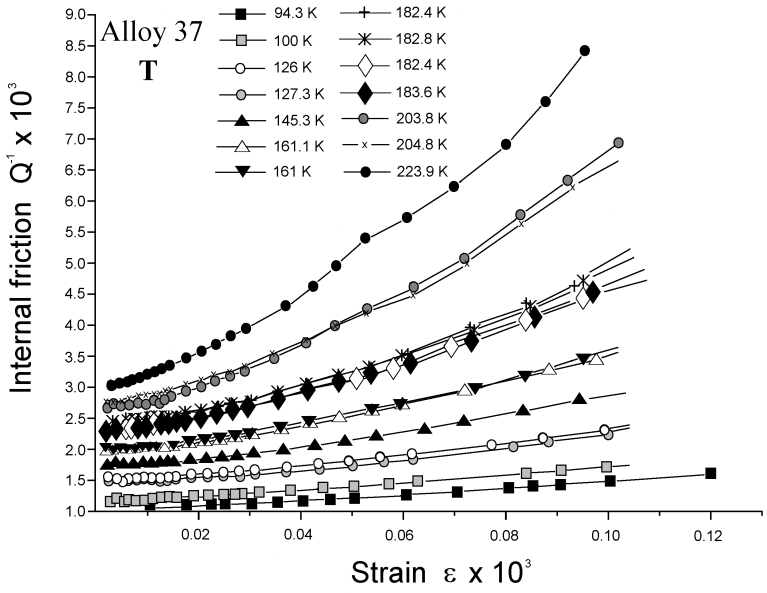

Figure 12. Strain-dependent internal friction (Q^{-1}) as a function of the temperature in Alloy 37. *Publication V.*

[Reprinted from Scripta Materialia Vol. **49** *V.G. Gavriljuk, O. Söderberg, V.V. Bliznuk, N.I. Glavatska and V.K. Lindroos,* **Martensitic Transformations and Mobility of Twin Boundaries in Ni_2MnGa Alloys Studied by Using Internal Friction**, p. 807. Copyright (2003), with permission from Elsevier.]

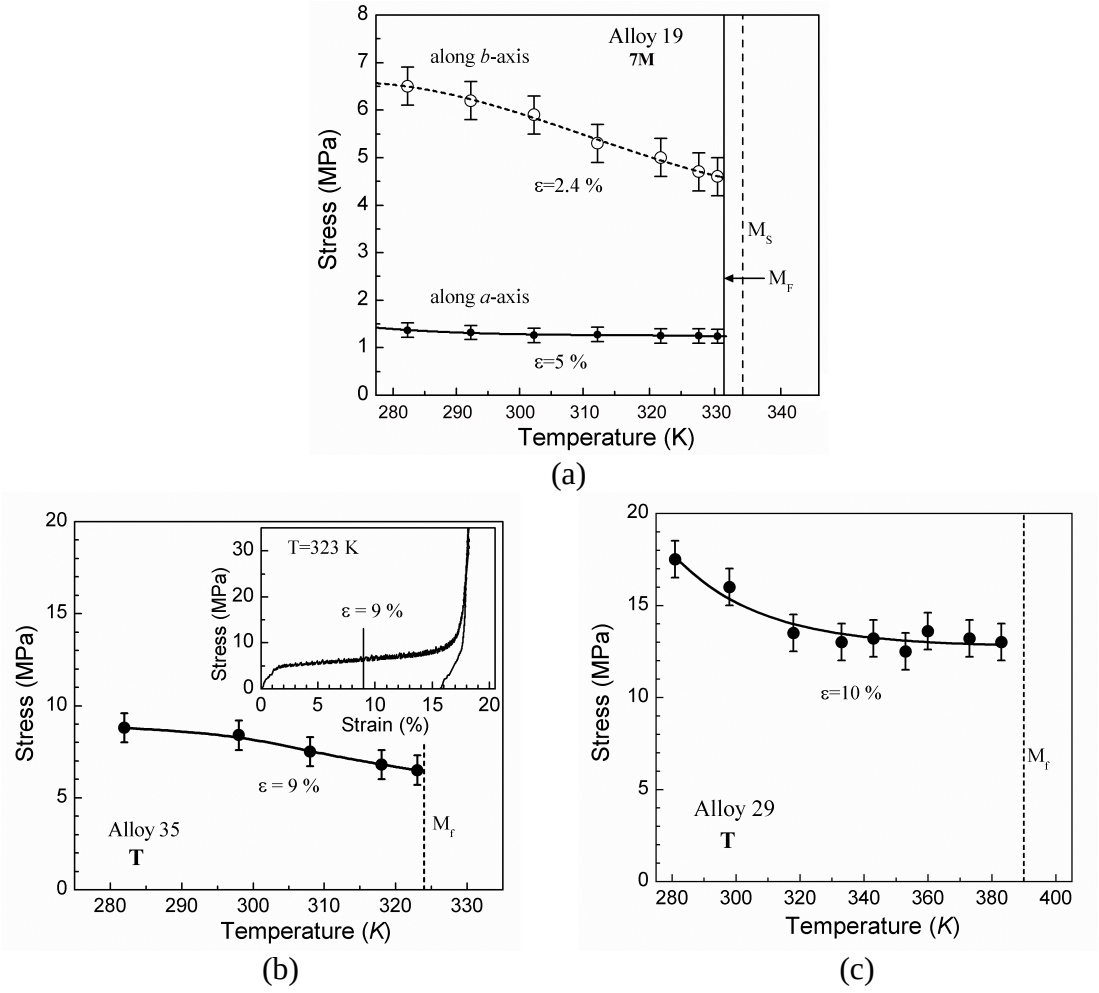

Figure 13. The effect of temperature on the twinning stress (a) in the **7M** structure of Alloy 19, (b) in the non-modulated **T** martensitic Alloy 35 and (c) in the non-modulated **T** martensitic Alloy 29. *Publications III, IV.*

[Reprinted from Materials Science and Engineering A Vol. **378/1-2** *A. Sozinov, A.A. Likhachev, N. Lanska, O. Söderberg, K. Ullakko, V.K. Lindroos*, **Stress- and magnetic-field-induced variant rearrangement in Ni-Mn-Ga single crystals with seven-layered martensitic structure**, p. 401. Copyright (2004), with permission from Elsevier.

Reprinted from Journal de Physique IV Vol. **115** *A. Sozinov, A.A. Likhachev, N. Lanska, O. Söderberg, K. Koho, K. Ullakko, V.K. Lindroos*, **Stress-induced variant rearrangement in Ni-Mn-Ga single crystals with nonlayered tetragonal martensitic structure**, p. 126. Copyright (2004), with permission from EDP Sciences.]

9. MAGNETO-MECHANICAL BEHAVIOUR OF SELECTED ALLOYS

The magneto-mechanical behaviour of the **7M** and **T** structures is studied in *Publications III* and *IV*. The realization of Eq. (4) is evaluated by studying the effect of the applied magnetic field on the twinning stress of the single-variant sample in compression at ambient temperature.

Alloys 15, 16 and 19 in *Publication IV* with the pure **7M** structure exhibit the MSME at 300 K (Figure 14a), but Alloy 17 with the mixed **7M**+**T** structure could not transform to the single-variant state and the large MFIS could not be obtained. When Alloy 19 was compressed to direction [100] and the magnetic field was applied along the [001] direction, the twinning stress was increased by the magnetic-field-induced stress $\Delta\sigma_{mag}$ (Figure 14b). The magnetic stress values of the half of the maximum strain ($\varepsilon \approx \varepsilon_0/2$) are plotted as a function of the applied field in Figure 14c. Here, the twinning stress is marked with the dashed line. When the magnetic field exceeds 0.5 T (approximately 400 kA/m), the magnetic induced strain exceeds the twinning stress and the MSME is possible. This agrees rather well with the MFIS results for Alloy 19 of Figure 14a, where the effect has already started at 0.4 T (approximately 320 kA/m). The maximum field-induced stress is slightly above 1.5 MPa (Figure 14c). This is in accordance with the theoretical value of 1.6 MPa obtained from Eq. (4) by using the maximum strain value of 10 % and the $K_U = 1.6 \times 10^5$ J/m^3 from [22].

The same type of magneto-mechanical study was carried out with Alloy 35 having the **T** structure (Figure 15), but now the test included more steps. At first, the twinning stress and the twinning strain were established with compression along the [001] direction – parallel to the long *c* axis (Figure 15a solid line). The original structure transformed to another martensite variant having the long *c* axis perpendicular to this first compression direction. Now the sample was rotated 90^o in order to have the same structure as at the beginning. When the magnetic field was applied perpendicular to the simultaneous compressive stress, the twinning stress increased about 1±0.2 MPa (Figure 15a, dashed line). During the second test, the magnetic field was switched on and off during the compressive testing to [100] direction (Figure 15b). Again the twinning stress increased with the magnetic field as in Figure 15a. The stress value returned to the normal when the field was switched off. The experimentally established magnetic-field-induced stress is in good agreement with the value $\sigma_{mag} = 1.1$ MPa obtained from Eq. (4) with a strain of 19 % and $|K_U| = 2.03 \times 10^5$ J/m^3 [57,58]. The same test was also carried out in the other direction of the easy magnetization of the **T** structure by applying the force along the [010] direction; however, the magnetic field did not increase the twinning stress at all (Figure 15c). The observed and calculated magnetic-field-induced stress values of the class 1 MPa were, however, much lower than the measured twinning stress – above 6 MPa in Figure 15. Consequently, there is no possibility of a giant magnetic shape memory effect according to Eq. (4) and, in practice, the measured magnetic-field-induced strain value is below 0.02 %.

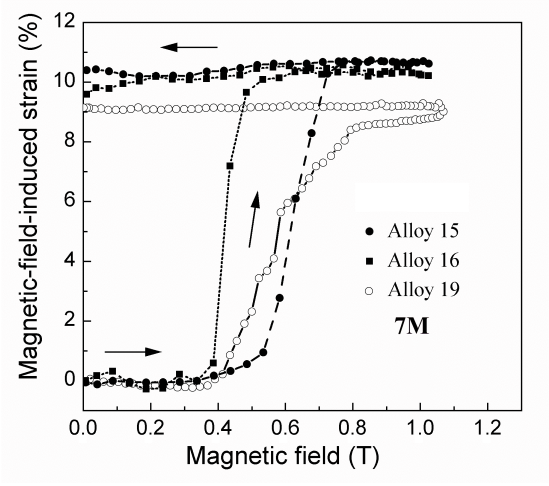

(a)

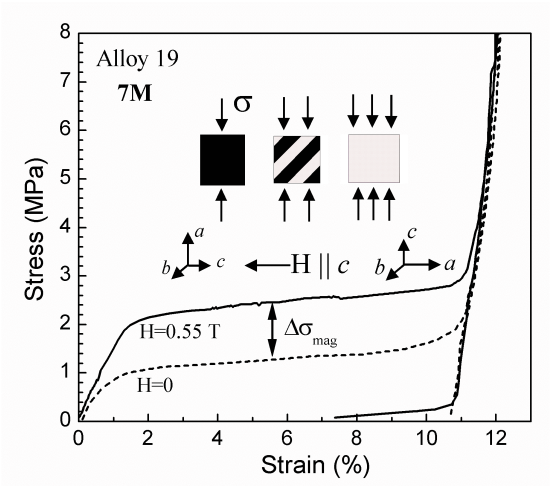

(b)

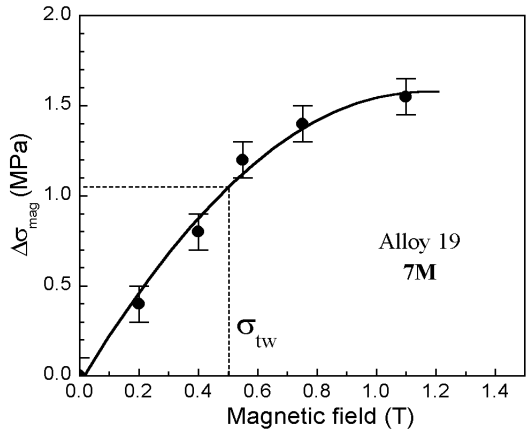

(c)

Figure 14. (a) The magnetic-field-induced strain (MFIS) of single-variant Alloys 15, 16 and 19 at 300 *K*. (b) The effect of the magnetic field on the twinning stress in Alloy 19 (*dashed line* without, and *solid line* with, the applied magnetic field H = 0.55 T). (c) The field dependence of the magnetic-field-induced stress increase $\Delta\sigma_{mag}$ at the strain value $\varepsilon \approx \varepsilon_0/2$; the dashed line shows the twinning stress of the alloy σ_{tw}. *Publication IV*.

[Reprinted from Materials Science and Engineering A Vol. **378/1-2** *A. Sozinov, A.A. Likhachev, N. Lanska, O. Söderberg, K. Ullakko, V.K. Lindroos*, **Stress- and magnetic-field-induced variant rearrangement in Ni-Mn-Ga single crystals with seven-layered martensitic structure**, pp. 401,402. Copyright (2004), with permission from Elsevier.]

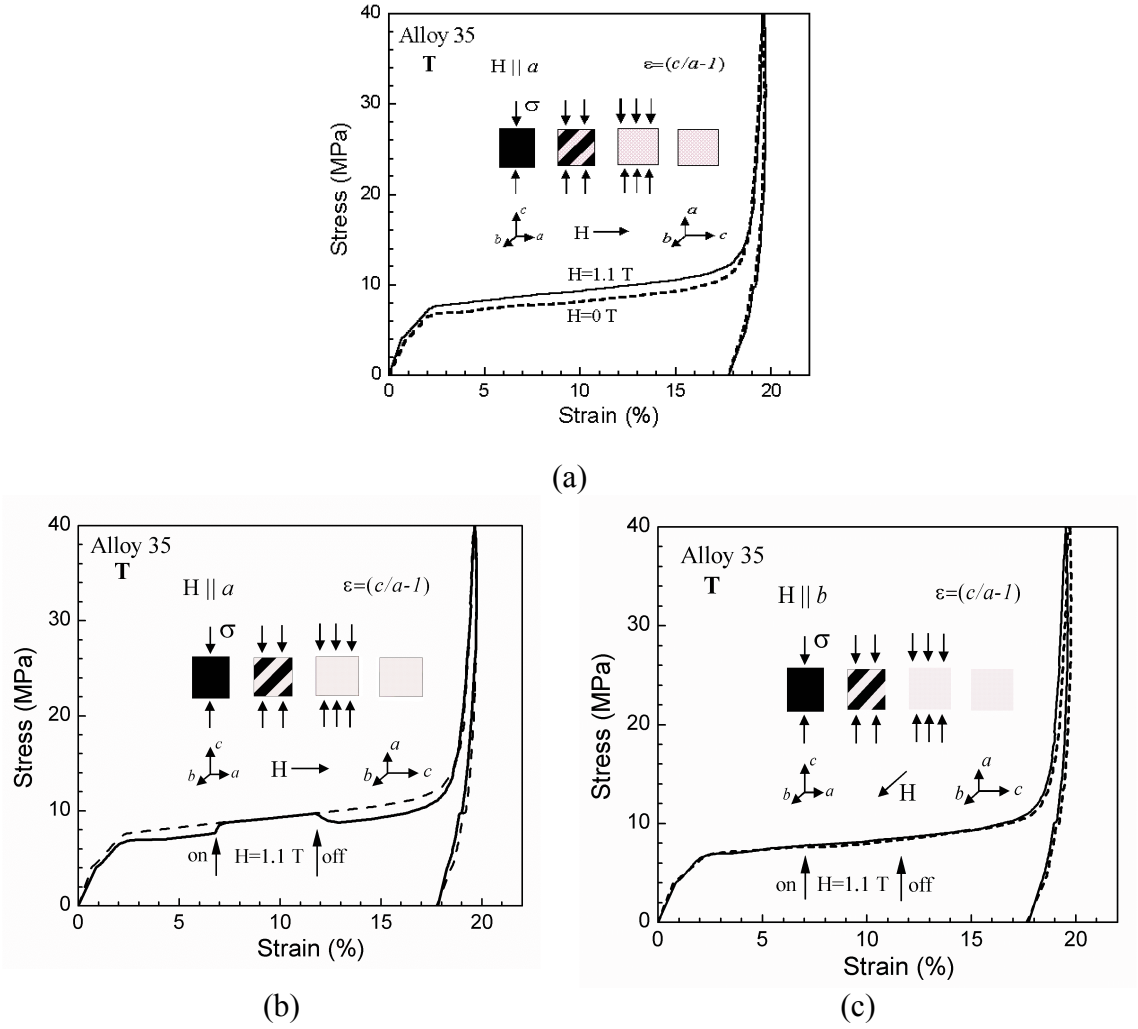

Figure 15. Stress-strain curves for compression of a single-variant Alloy 35 along the [001] direction at 300 K. Test with magnetic field applied along the [100] direction: (a) – without magnetic field (dashed line) and with the magnetic field applied (solid line) and (b) – magnetic field was switched on and off during the compression test, dashed line shows the stress-strain curve under continuously applied magnetic field. Test with magnetic field applied along the [010] direction (c) – magnetic field was switched on and switched off during the compression test (solid line), dashed line shows the stress-strain curve without magnetic field. *Publication III*.

[Reprinted from Journal de Physique IV Vol. **115** *A. Sozinov, A.A. Likhachev, N. Lanska, O. Söderberg, K. Koho, K. Ullakko, V.K. Lindroos,* **Stress-induced variant rearrangement in Ni-Mn-Ga single crystals with nonlayered tetragonal martensitic structure**, p. 127. Copyright (2004), with permission from EDP Sciences.]

10. CONCLUSIONS

Altogether 37 ternary Ni-Mn-Ga alloys with three different crystal structures were introduced in the present thesis. Of these, alloys with the seven layered nearly orthorhombic martensitic (**7M**) or the non-layered tetragonal martensitic (**T**) structures were studied in more detail. Three new alloys with the **7M** structure at ambient temperatures (Alloys 15, 16 and 17 in Table 2), as well as three new alloys showing the **7M** structure above ambient temperature and the **T** structure at ambient temperature (Alloys 30, 33 and 34 in Table 2), were presented.

The detailed information as to the temperatures at which certain ferromagnetic martensite structure occurs is important for establishing the service temperature limits of the magnetic shape memory effect. The structural and magnetic transitions were applied by dividing the studied **7M** and **T** alloys into six main groups:

A	**7M ambient,**		***D***	**T high,**
B	**7M above,**		***E***	**T low,**
C	**7M co-transition**	and	***F***	**T co-transition.**

In the groups ***A***, ***B***, ***D*** and ***E***, the structural and magnetic transitions are clearly separated from each other, while in the groups ***C*** and ***F*** they co-occur, resulting in a hysteresis of the Curie point. This hysteresis is explained with co-occurring structural transformations and with the different Curie points of the phases involved. In addition to the existing suggestion that the cubic parent phase and the tetragonal martensitic phase have different magnetic transition points, the present thesis shows that both the martensitic phases, the **7M** and the **T**, have their own Curie points.

The present work confirms that the **7M ambient** alloys show the magnetic shape memory effect (MSME) at ambient temperature, if they are in the single-variant state. It is possible to obtain the single-variant structure in a one-phase alloy by pre-training three successive compressions to two crystallographic orientations. The present work confirms by the magneto-mechanical testing that the magnetic-field-induced force exceeds the twinning stress of the single-variant material. Consequently, the theoretical requirement for MSME is fulfilled and the crystallographically limited maximum magnetic-field-induced strain of 10 % can be obtained in these alloys. As the MSME has been observed in the **7M ambient** alloys, there might be the possibility of it being observed in the **7M above** and the **7M co-transition** alloys also. In both of them, the pre-straining temperature, the storage and the MSM service temperatures should be carefully controlled to ensure the **7M** structure. However, the MSME of these groups needs further study since it is also affected by, for example, the effect of temperature on the magnetically induced stress.

By applying different pre-straining methods and by the magneto-mechanical testing, the current thesis confirms that, in the non-modulated **T** phase, the magnetic-field-induced MSM effect is not possible. The single-variant structure is possible with three successive compressions to three different crystallographic orientations or by tensile/compressive cycling. However, in both methods, the twinning stress of the material exceeds 6 MPa even at elevated temperatures. This value clearly exceeds the magnetically induced stress of the phase – about 1 MPa – and, consequently, the MSME is not possible.

LIST OF REFERENCES

[1] K. Otsuka and C.M. Wayman *Shape Memory Materials*. Cambridge University Press 1998, 284 p.

[2] S. Trolier-McKinstry and R.E. Newnham *Sensors, Actuators and Smart Materials.* MRS Bulletin **18** (1993) 27-33.

[3] T. Takagi *Recent research on intelligent materials*. Journal of Intelligent Material Systems and Structures **7** (1996) 346-352.

[4] R.C. O'Handley and S.M. Allen *Shape memory alloys, magnetically activated ferromagnetic shape- memory materials*. In: M. Schwartz (Ed.) Encyclopedia of Smart Materials, John Wiley and Sons, New York, 2001, pp. 936-951.

[5] A.N. Vasil'ev, V.D. Buchel'nikov, T. Takagi, V.V. Khovailo and E.I. Estrin *Shape memory ferromagnets*. Physics-Uspekhi **46 (6)**, 559-588; http://arxiv.org/archive/cond-mat/0311433, 19 Nov 2003.

[6] O. Söderberg, A. Sozinov, Y. Ge, S.-P. Hannula and V.K. Lindroos *Giant Magnetostrictive Materials*. In: J. Buschow (Ed.) Handbook on Magnetic Materials. Elsevier Science, Amsterdam (to be published 2005).

[7] K. Ullakko *Magnetically controlled shape memory alloys: A new class of actuator materials.* Journal of Materials Engineering and Performance **5** (1996) 405-409.

[8] K. Ullakko, J.K. Huang, C. Kantner, R.C. O'Handley and V.V. Kokorin, *Large magnetic-field-induced strains in Ni_2MnGa single crystals*. Applied Physics Letters **13** (1996) 1966-1968.

[9] K. Ullakko, J.K. Huang, V.V. Kokorin and R.C. O'Handley *Magnetically controlled shape memory effect in Ni_2MnGa intermetallics*. Scripta Materialia **36** (1997) 1133-1138.

[10] R. Tickle and R. D. James *Magnetic and magnetomechanical properties of Ni_2MnGa*. Journal of Magnetism and Magnetic Materials **195** (1999) 627-638.

[11] G.H. Wu, C.H. Yu, L.Q. Meng, J.L. Chen, F.M. Yang, S.R. Qi, W.S. Zhan, Z. Wang, Y.F. Zheng and L.C. Zhao *Giant magnetic-field-induced strains in Heusler alloy NiMnGa with Modified Composition*. Applied Physics Letters **75** (1999) 2990-2992.

[12] S.J. Murray, M. Marioni, S.M. Allen, R.C. O'Handley and T.A. Lograsso *6% magnetic-field-induced strain by twin-boundary motion in ferromagnetic Ni-Mn-Ga*. Applied Physics Letters **77** (2000) 886-888.

[13] O. Heczko, A. Sozinov and K. Ullakko *Giant field-induced reversible linear strain in magnetic shape memory NiMnGa at room temperature.* IEEE Transactions on Magnetics **36** (2000) 3266-3268.

[14] Y. Ezer, A. Sozinov, G. Kimmel, P. Yakovenko, K. Ullakko and V. K. Lindroos *Large Magnetic-Field-Induced Strains in Textured Polycrystalline Ni-Mn-Ga at Room Temperature.* In: A.S. Khan, H. Zhang and Y. Yuan (Eds.) Proceeding of PLASTICITY 2000, NEAT PRESS, Maryland, 2000, pp. 522-524.

[15] A.A. Likhachev and K. Ullakko *Magnetic-field-controlled twin boundaries motion and giant magneto-mechanical effects in Ni-Mn-Ga shape memory alloy*. Physics Letters A **275** (2000) 142-151.

[16] A. Sozinov, P. Yakovenko and K. Ullakko *Large magnetic-field-induced strains in Ni-Mn-Ga alloys due to redistribution of martensite variants*. Materials Science Forum **373-376** (2001) 35-40.

[17] R.C. O'Handley, S.J. Murray, M. Marioni, P.G. Tello and S.M. Allen *Giant magnetic-field-induced strain in Ni-Mn-Ga crystals: experimental results and modelling*. Journal of Magnetism and Magnetic Materials **226-230** (2001) 945-947.

[18] K. Ullakko, Y. Ezer, A. Sozinov, G. Kimmel, P. Yakovenko and V.K. Lindroos *Magnetic-field-induced strains in polycrystalline Ni-Mn-Ga at room temperature*. Scripta Materialia **44** (2001) 475-480.

[19] Y. Ezer *Magnetic Shape Memory (MSM) Effect in Ni-Mn-Ga Alloy*. Thesis for Doctor of Technology at Helsinki University of Technology, Laboratory of Physical Metallurgy and Materials Science, Acta Polytechnica 2002. 29 p.

[20] M.A. Marioni, D. Bono, R.C. O'Handley and S.M. Allen *Pulsed magnetic field actuation of single-crystalline ferromagnetic shape memory alloy Ni-Mn-Ga*. In: C.S. Lynch (Ed.) Proceedings of SPIE, **4699** (2002) 191-194.

[21] C.P. Henry, J. Feuchtwanger, D. Bono, R.C. O'Handley and S.M. Allen *AC magnetic-field-induced strain of single-crystal Ni-Mn-Ga*. In: C.S. Lynch (Ed.) Proceedings of SPIE, **4699** (2002) 164-171.

[22] A. Sozinov, A. A. Likhachev, N. Lanska and K. Ullakko *Giant magnetic-field-induced strain in NiMnGa seven-layered martensitic phase*. Applied Physics Letters **80** (2002) 1746-1748.

[23] F. Heusler, W. Starck and E. Haupt *Magnetisch-chemische Studien: I. Über die Synthese ferromagnetischer Mangan-legierungen*. Verhandlungen der Deutschen Physikalischen Gesellschaft **5** (1903) 220-223.

[24] F. A. Hames (1960) *Ferromagnetic-alloy phases near the compositions Ni_2MnIn, Ni_2MnGa, Co_2MnGa, Pd_2MnSb, and PdMnSb*. Journal of Applied Physics **31** (1960) 370S-371S.

[25] M. Elfazani, M. DeMarco, S. Jha, G.M. Julian and J.W. Blue *Hyperfine magnetic field at cadmium impurity in Heusler alloys nickel-manganese-gallium (Ni_2MnGa), nickel-manganese-indium (Ni_2MnIn), copper-manganese-indium (Cu_2MnIn), and gold-manganese-indium (Au_2MnIn)*. Journal of Applied Physics **52** (1981) 2043-2045.

[26] C. Mitros, S. Yehia, S. Kumar, S. Jha, M. DeMarco, D. Mitchell, G.M. Julian and R.A. Dunlap *Hyperfine magnetic field measurements in Heusler alloys nickel-manganese-gallium (Ni_2MnGa), palladium-manganese-tin (Pd_2MnSn), and ruthenium-iron-tin (Ru_2FeSn)*. Hyperfine Interactions **34** (1987) 419-422.

[27] T. Kanomata, K. Shirakawa and T. Kaneko *Effect of hydrostatic pressure on the Curie temperature of the Heusler alloys nickel-manganese-Z (Ni_2MnZ) (Z = aluminum, gallium, indium, tin and antimony)*. Journal of Magnetism and Magnetic Materials **65** (1987) 76-82.

[28] S. Fujii, S. Ishida and S. Asano *Electronic structure and lattice transformation in nickel-manganese-gallium (Ni_2MnGa) and cobalt-niobium-tin (Co_2NbSn)*. Journal of the Physical Society of Japan **58** (1989) 3657-3665.

[29] J. Soltys *Magnetic properties of the Heusler alloy nickel-manganese-gallium (Ni_2MnGa)*. Acta Physica Polonica A **46** (1974) 383-384.

[30] J. Soltys *Effect of heat treatment on the atomic arrangement and the magnetic properties in nickel-manganese-gallium (Ni_2MnGa).* Acta Physica Polonica A **47** (1975) 521-523.

[31] P.J. Webster, K.R.A. Ziebeck, S.L. Town and M.S. Peak *Magnetic order and phase transformation in Ni_2MnGa.* Philosophical Magazine B **49** (1984) 295-310.

[32] V.V. Kokorin and V.A. Chernenko *Martensitic transformation in ferromagnetic Heusler alloy.* Fizika Metallov i Metallovedenie **68** (1989) 1157-1161.

[33] V.V. Kokorin, I.A. Osipenko and V. Chernenko *Alloy with shape memory effect.* Sovjet Union patent SU1611980, publication date 1990-12-07.

[34] V. A. Chernenko, V. V. Kokorin and I. N. Vitenko *The development of new ferromagnetic shape memory alloys in Ni-Mn-Ga system.* Scripta Metallurgica et Materialia **33** (1995) 1239-1244.

[35] A.N. Vasil'ev, A.D. Bozhko, V.V. Khovailo, I.E. Dikshtein, S.G. Shavrov, V.D. Buchelnikov, M. Matsumoto, S. Suzuki, T. Takagi and J. Tani *Structural and magnetic phase transitions in shape-memory alloys $Ni_{2+x}Mn_{1-x}Ga$.* Physical Review B **59** (1999) 1113-1120.

[36] V.A. Chernenko *Compositional instability of beta-phase in Ni-Mn-Ga alloys.* Scripta Materialia **40** (1999) 523-527.

[37] S.K. Wu and S.T. Yang *Effect of composition on transformation temperatures of Ni-Mn-Ga shape memory alloys.* Materials Letters **57** (2003) 4291-4296.

[38] C. Jiang, G. Feng, S. Gong and H. Xu *Effect of Ni excess on phase transformation temperatures of NiMnGa alloys.* Materials Science and Engineering A **342** (2003) 231-235.

[39] X. Jin, M. Marioni, D. Bono, S.M. Allen, R.C. O'Handley and T.Y. Hsu *Empirical mapping of Ni-Mn-Ga properties with composition and valence electron concentration.* Journal of Applied Physics **91** (2002) 8222-8224.

[40] F. Albertini, L. Pareti, A. Paoluzi, L. Morelon, P.A. Algarabel, M.R. Ibarra and L. Righi *Compositional and temperature dependence of the magnetocrystalline anisotropy in $Ni_{2+x}Mn_{1+y}Ga_{1+z}$ $(x+y+z=0)$ Heusler alloys.* Applied Physics Letters **81** (2002) 4032-4034.

[41] I. Takeuchi, O.O. Famodu, J.C. Read, M.A. Aronova, K.S. Chang, C. Craciunescu, S.E. Lofland, M. Wuttig, F.C. Wellstood, L. Knauss and A. Orozco *Identification of novel compositions of ferromagnetic shape-memory alloys using composition spreads.* Nature Materials **2** (2003) 180-184.

[42] D.L. Schlagel, Y.L. Wu, W. Zhang and T.A. Lograsso *Chemical segregation during bulk single crystal preparation of Ni-Mn-Ga ferromagnetic shape memory alloys.* Journal of Alloys and Compounds **312** (2000) 77-85.

[43] C. Wedel and K. Itagaki *High-Temperature Phase Relations in the Ternary Ga-Mn-Ni System.* Journal of Phase Equilibria **22** (2001) 324-330.

[44] R.W. Overholser, M. Wuttig and D.A. Neumann *Chemical ordering in Ni-Mn-Ga Heusler alloys.* Scripta Materialia **40** (1999) 1095-1102.

[45] V.V. Khovailo, T. Takagi, A.N. Vasilev, H. Miki, M. Matsumoto and R. Kainuma, *On order-disorder ($L2_1 \rightarrow B2'$) phase transition in $Ni_{2+x}Mn_{1-x}Ga$ Heusler alloys*. Physica Status Solidi (a) **183** (2001) R1-R3.

[46] M. Kreissl, K.U. Neumann, T. Stephens and K.R.A. Ziebeck *The influence of atomic order on the magnetic and structural properties of the ferromagnetic shape memory compound Ni_2MnGa.* Journal of Physics **15** (2003) 3831-3839.

[47] K. Tsuchiya, D. Ohtoyo, M. Umemoto and H. Ohtsuka *Effect of isothermal aging on martensitic transformation in Ni - Mn - Ga alloys.* Transactions of the Materials Research Society of Japan **25** (2000) 521-523.

[48] M. Pasquale, C. Sasso, S. Besseghini, F. Passaretti, E. Villa and A. Sciacca *NiMnGa polycrystalline magnetically activated shape memory alloys*. IEEE Transactions on Magnetics **36** (2000) 3263-3265.

[49] S. Besseghini, M. Pasquale, F. Passaretti, A. Sciacca and E. Villa *NiMnGa polycrystalline magnetically activated shape memory alloy: a calorimetric investigation.* Scripta Materialia **44** (2001) 2681-2687.

[50] V. Chernenko, V. L'Vov, E. Césari, J. Pons, R. Portier and S. Zagorodnyuk *New aspects of structural and magnetic behaviour of martensites in Ni-Mn-Ga alloys.* Materials Transactions JIM **43** (2002) 856-860.

[51] O. Söderberg, K. Koho, T. Sammi, X.W. Liu, A. Sozinov, N. Lanska and V.K. Lindroos *Effect of the selected alloying on Ni-Mn-Ga alloys*, Materials Science and Engineering A **378/1-2** (2004) 386-393.

[52] V.A. Chernenko, V. L'Vov, J. Pons and E. Césari *Superelasticity in high-temperature Ni-Mn-Ga alloys.* Journal of Applied Physics **93** (2003) 2394-2399.

[53] K. Koho *Behaviour of Some NiMnGa Shape Memory Alloys under Compression.* Thesis for Master of Science degree, Helsinki University of Technology, Department of Materials Science and Rock Engineering, 2002. 67 p. (In Finnish)

[54] J. Pons, V.A. Chernenko, R. Santamarta and E. Césari *Crystal structure of martensitic phases in Ni-Mn-Ga shape memory alloys.* Acta Materialia **48** (2000) 3027-3038.

[55] K. Tsuchiya, H. Nakamura, D. Ohtoyo, H. Nakayama, H. Ohtsuka and M. Umemoto *Composition dependence of phase transformations and microstructures in Ni-Mn-Ga ferromagnetic shape memory alloys.* Proceedings of ISAEM 2000: 2nd International Symposium on Designing, Processing and Properties of Advanced Engineering Materials; Guilin; China; 20-21 Oct. 2000. 2001.pp. 409-414.

[56] O. Heczko, L. Straka and K. Ullakko *Relation between structure, magnetization process and magnetic shape memory effect of various martensites occurring in Ni-Mn-Ga alloys.* Journal de Physique IV **112** (2003) 959-962.

[57] A. Sozinov, A.A. Likhachev and K. Ullakko *Magnetic and magnetomechanical properties of Ni-Mn-Ga alloys with easy axis and easy plane of magnetization.* In: C.S. Lynch (Ed.) Proceedings of SPIE, **4333** (2001) 189-196.

[58] A. Sozinov, A.A. Likhachev and K. Ullakko *Crystal structures and magnetic anisotropy properties of Ni-Mn-Ga martensitic phases with giant magnetic-field-induced strain.* IEEE Transactions on Magnetics **38** (2002) 2814-2816.

[59] K. Koho, J. Vimpari, L. Straka, N. Lanska, O. Söderberg, O. Heczko, K. Ullakko and V.K. Lindroos *Behaviour of Ni-Mn-Ga alloys under mechanical stress.* Journal de Physique IV **112** (2003) 943-946.

[60] X.W. Liu, O. Söderberg, Y. Ge, A. Sozinov and V.K. Lindroos *Corrosion behavior of NiMnGa shape-memory alloy.* Materials Science Forum **394-395** (2002) 565-568.

[61] X.W. Liu, O. Söderberg, Y. Ge, N. Lanska, K. Ullakko and V.K. Lindroos *On the corrosion of non-stoichiometric martensitic Ni-Mn-Ga alloys.* Journal de Physique IV **112** (2003) 935-938.

[62] Z. Nishiyama, *Martensitic Transformation* / Zenji Nishiyama, (Eds.) Morris E. Fine, M. Meshii and C.M. Wayman, Academic Press, New York London 1978. 467 p.

[63] L. Kaufman and M. Hillert *Thermodynamics of Martensitic Transformations*. In Martensite, Eds. G.B. Olson and W.S. Owen, ASM International 1992. pp. 41-58.

[64] S. Wirth, A. Leithe-Jasper, A.N. Vasil'ev and J.M.D. Coey *Structural and magnetic properties of Ni_2MnGa.* Journal of Magnetism and Magnetic Materials **167** (1997) L7-L11.

[65] M. Matsumoto, T. Takagi, J. Tani, T. Kanomata, N. Muramatsu and A.N. Vasil'ev *Phase Transformation of Heusler type $Ni_{2+x}Mn_{1-x}Ga$ (x=0~0.19).* Materials Science Engineering A **273-275** (1999) 326-328.

[66] I. Dikshtein, V. Koledov, V. Shavrov, A. Tulaikova, A. Cherechukin, V. Buchelnikov, V. Khovailo, M. Matsumoto, T. Takagi and J. Tani *Phase transitions in intermetallic compounds Ni-Mn-Ga with shape memory effect.* IEEE Transactions on Magnetics **35** (1999) 3811-3813.

[67] L. Mañosa and A. Planes *Structural and magnetic phase transitions in Ni-Mn-Ga shape-memory alloys.* Advances in Solid State Physics **40** (2000) 361-374.

[68] W.H. Wang, F.X. Hu, J.L. Chen, Y.X. Li, Z. Wang, Z.Y. Gao, Y.F. Zheng, L.C. Zhao, G.H. Wu and W.S. Zhan *Magnetic properties and structural phase transformations of NiMnGa alloys.* IEEE Transactions on Magnetics **37** (2001) 2715-2717.

[69] G. Feng, C. Jiang, T. Liang and H. Xu *Magnetic and structural transition of $Ni_{50+x}Mn_{25-x/2}Ga_{25-x/2}$ (x=2-5) alloys.* Journal of Magnetism and Magnetic Materials **248** (2002) 312-317.

[70] V.V. Kokorin, I.A. Osipenko and T.V. Shirina *Phase transitions in alloys $Ni_2MnGa_xIn_{1-x}$.* Physics of Metals and Metallography (Russia) **67** (1989) 173-176.

[71] K. Endo, K. Ooiwa and A. Shinogi *Structural phase transitions and magnetism of $Ni_2Mn_{1-x}V_xGa$ and $(Co_{1-y}Ni_y)_2NbSn$.* Journal of Magnetism and Magnetic Materials **104-107** (1992) 2013-2014.

[72] K. Tsuchiya, H. Nakamura, M. Umemoto and H. Ohtsuka *Effect of fourth elements on phase transformations in Ni-Mn-Ga Heusler alloys.* Transactions of the Materials Research Society of Japan **25** (2000) 517-519.

[73] H. Nakamura, K. Tsuchiya and M. Umemoto *Martensitic transformation behavior in $Ni_{50}Mn_{25-x}Ga_{25}Co_x$ alloy.* Transactions of the Materials Research Society of Japan **26** (2001) 287-289.

[74] A.A. Cherechukin, I.E. Dikshtein, D.I. Ermakov, A.V. Glebov, V.V. Koledov, D.A. Kosolapov, V.G. Shavrov, A.A. Tulaikova, E.P. Krasnoperov and T. Takagi *Shape memory effect due to magnetic field-induced thermaelatic martensitic transformation in polycrystalline Ni-Mn-Fe-Ga alloy.* Physics Letters A **291** (2001) 175-183.

[75] V.V. Khovailo, T. Abe, V.V. Koledov, M. Matsumoto, H. Nakamura, R. Note, M. Ohtsuka, V.G. Shavrov and T. Takagi T *Influence of Fe and Co on phase transitions in Ni-Mn-Ga alloys.* Materials Transactions JIM **44** (2003) 2509-2512.

[76] X. Lu, X. Chen, L. Qiu and Z. Qin *Martensitic transformation of Ni-Mn-Ga (C,Si,Ge) Heusler alloys.* Journal de Physique IV **112** (2003) 917-920.

[77] K. Yamaguchi, S. Ishida and S. Asano *Valence electron concentration and phase transformations of shape memory alloys Ni-Mn-Ga-X.* Materials Transactions JIM **44** (2003) 204-210.

[78] A.A. Cherechukin, T. Takagi, H. Miki, M. Matsumoto and M. Ohtsuka *Influence of three-dimensional transition elements on magnetic and structural phase transitions of Ni-Mn-Ga alloys.* Journal of Applied Physics **95** (2004) 1740-1742.

[79] K. Koho, O. Söderberg, N. Lanska, Y. Ge, X. Liu, L. Straka, J. Vimpari and V.K. Lindroos *Effect of the chemical composition to martensitic transformation in Ni-Mn-Ga-Fe alloys*, Materials Science and Engineering A **378/1-2** (2004) 384-388.

[80] J. Enkovaara *Atomistic simulations of magnetic shape memory alloys*. Laboratory of Physics Helsinki University of Technology, Dissertation 119 (2003). 47 p.

[81] V.V. Martynov and V.V. Kokorin *The crystal structure of thermally- and stress-induced martensites in nickel-manganese-gallium (Ni_2MnGa) single crystals.* Journal de Physique III **2** (1992) 739-749.

[82] V.V. Martynov *X-ray diffraction study of thermally and stress-induced phase transformations in single crystalline Ni-Mn-Ga alloys.* Journal de Physique IV **5** (1995) 91-99.

[83] V.A. Chernenko, C. Seguí, E. Césari, J. Pons and V.V. Kokorin *Sequence of martensitic transformations in Ni-Mn-Ga alloys.* Physical Review B **57** (1999) 2659-2662.

[84] K. Tsuchiya, A. Ohashi, D. Ohtoyo, H. Nakayama, M. Umemoto and P.G. McCormick *Phase transformations and magnetostriction in Ni-Mn-Ga ferromagnetic shape memory alloys.* Materials Transactions JIM **41** (2000) 938-942.

[85] C. Jiang, G. Feng and H. Xu *Co-occurrence of magnetic and structural transitions in the Heusler alloy $Ni_{53}Mn_{25}Ga_{22}$.* Applied Physics Letters **80** (2002) 1619-1621.

[86] C. Jiang, T. Liang, H. Xu, M. Zhang and G. Wu (2002) *Superhigh strains by variant reorientation in the nonmodulated ferromagnetic NiMnGa alloys.* Applied Physics Letters **81** (2002) 2818-2820.

[87] X. Lu, Z. Qin and X. Chen *Two-step martensitic transformation characteristics of polycrystalline NiMnGa Heusler alloys.* Materials Science Forum **394-395** (2002) 549-552.

[88] V.A. Chernenko, J. Pons, C. Seguí and E. Césari *Premartensitic phenomena and other phase transformations in Ni-Mn-Ga alloys studied by dynamical mechanical analysis and electron diffraction.* Acta Materialia **50** (2002) 53-60.

[89] V.A. Chernenko, V. L'Vov, J. Pons and E. Césari *Superelasticity in high-temperature Ni-Mn-Ga alloys.* Journal of Applied Physics **93** (2003) 2394-2399.

[90] V. Soolshenko, N. Lanska and K. Ullakko *Structure and twinning stress of martensites in non-stoichiometric Ni_2MnGa single crystal.* Journal de Physique IV France **112** (2003) 947-950.

[91] O. Heczko, N. Lanska, O. Söderberg and K. Ullakko *Temperature variation of structure and magnetic properties of Ni-Mn-Ga magnetic shape memory alloys.* Journal of Magnetism and Magnetic Materials **242-245** (2002) 1446-1449.

[92] G. Fritsch, V.V. Kokorin, V.A. Chernenko, A. Kempf and I.K. Zasimchuk *Martensitic transformation in Ni-Mn-Ga alloys.* Phase Transitions **57** (1996) 233-240.

[93] Y. Ge, O. Söderberg, N. Lanska, A. Sozinov, K. Ullakko and V.K. Lindroos *Crystal structure of three Ni-Mn-Ga alloys in powder and bulk materials.* Journal de Physique IV **112** (2003) 921-924.

[94] N. Glavatska, G. Mogilniy, I. Glavatsky, S. Danilkin, D. Hohlwein, A. Beskrovnij, O. Söderberg and V.K. Lindroos *Temperature dependence of martensite structure and its effect on magnetic-field-induced strain in Ni_2MnGa magnetic shape memory alloys.* Journal de Physique IV **112** (2003) 963-967.

[95] Y. Ma, S. Awaji, K. Watanabe, M. Matsumoto and N. Kobayashi *X-ray diffraction study of the structural phase transition of Ni_2MnGa alloys in high magnetic fields.* Solid State Communications **113** (2000) 671-676.

[96] N. Glavatska, G. Mogylny, I. Glavatsky, A. Tyshchenko, O. Söderberg and V.K. Lindroos *Temperature dependence of magnetic shape-memory effect and martensitic structure of NiMnGa alloy.* Materials Science Forum **394-395** (2002) 537-540.

[97] O. Heczko, L. Straka, N. Lanska, K. Ullakko and J. Enkovaara *Temperature dependence of magnetic anisotropy in Ni-Mn-Ga alloys exhibiting giant field-induced strain.* Journal of Applied Physics **91** (2002) 8228-8230.

[98] L. Straka and O. Heczko *Magnetic anisotropy in Ni-Mn-Ga martensites.* Journal of Applied Physics **93** (2003) 8636-8638.

[99] A. Sozinov, A.A. Likhachev, N. Lanska, K. Ullakko and V.K. Lindroos *Crystal structure, magnetic anisotropy, and mechanical properties of seven-layered martensite in Ni-Mn-Ga.* In: C.S. Lynch (Ed.) Proceedings of SPIE, **4699** (2002) 195-205.

[100] N. Lanska and K. Ullakko *Microstructure change in Ni-Mn-Ga seven-layered martensite connected with MSM effect.* Journal de Physique IV **112** (2003) 925-928.

[101] V.A. Chernenko, E. Césari, J. Pons and C. Seguí *Phase transformations in rapidly quenched Ni-Mn-Ga alloys.* Journal of Materials Research **15** (2000) 1496-1504.

[102] J. Pons, R. Santamarta, E. Césari and V.A. Chernenko *Martensitic structures in Ni-Mn-Ga.* Applied Crystallography **18th** (2001) 186-199.

[103] J. Pons, R. Santamarta, V.A. Chernenko and E. Césari *HREM study of different martensitic phases in Ni-Mn-Ga alloys.* Materials Chemistry and Physics **81** (2003) 457-459.

[104] B.D. Cullity *Introduction to magnetic materials* Addison-Wesley, Reading (MA), London 1972. 666 p.

[105] V.V. Khovailo, T. Takagi, J. Tani, R.Z. Levitin, A.A. Cherechukin, M. Matsumoto and R. Note *Magnetic properties of $Ni_{2.18}Mn_{0.82}Ga$ Heusler alloys with a coupled magnetostructural transition.* Physical Review B **65** (2002) 092410 1-4.

[106] O. Heczko and L. Straka *Temperature dependence and temperature limits of magnetic shape memory effect.* Journal of Applied Physics **94** (2003) 7139-7143.

[107] R.C. O'Handley *Model for strain and magnetization in magnetic shape-memory alloys.* Journal of Applied Physics **83** (1998) 3263-3270.

[108] A.A. Likhachev, A. Sozinov and K. Ullakko *Influence of external stress on the reversibility of magnetic-field-controlled shape memory effect in Ni-Mn-Ga*. In: C.S. Lynch (Ed.) Proceedings of SPIE, **4333** (2001) 197-206.

[109] R.D. James and M. Wuttig *Magnetostriction of martensite.* Philosophical Magazine A **77** (1998) 1273-1299.

[110] R.C. O'Handley, S.J. Murray, M. Marioni, H. Nembach and S.M. Allen *Phenomenology of giant magnetic-field-induced strain in ferromagnetic shape-memory materials (invited).* Journal of Applied Physics **87** (2000) 4712-4717.

[111] L. Hirsinger and C. Lexcellent *Internal variable model for magneto-mechanical behaviour of ferromagnetic shape memory alloys Ni-Mn-Ga.* Journal de Physique IV **112** (2003) 977-980.

[112] H. Kato and K. Sasaki *Straining of magnetic shape memory martensite by uniform magnetic field.* Scripta Materialia **48** (2003) 31-35.

[113] D.I. Paul, J. Marquiss and D. Quattrochi *Theory of magnetization. Twin boundary interaction in ferromagnetic shape memory alloys.* Journal of Applied Physics **93** (2003) 4561-4565.

[114] A. Sozinov, A.A. Likhachev, N. Lanska, K. Ullakko and V.K. Lindroos *10% magnetic-field-induced strain in Ni-Mn-Ga seven-layered martensite*. Journal de Physique IV **112** (2003) 955-958.

[115] J. Seuranen *X-ray Diffraction Structure Studies of Shape Memory Ni-Mn-Ga Alloys*, Thesis for Master of Science degree, Helsinki University of Technology, Department of Materials Science and Rock Engineering, 2003. 150 p.

[116] A. Jääskeläinen *Magnetomechanical properties of Ni_2MnGa* Thesis for Master of Science degree, Helsinki University of Technology, Department of Materials Science and Rock Engineering, 2001. 67 p.

[117] Y. Ge, E. Heikinheimo, O. Söderberg and V.K. Lindroos *Microanalysis of one NiMnGa alloy*. In: J. Keränen and K. Sillanpää (Eds.) Proceedings of Scandem 2002, The 53rd Annual Meeting of The Scandinavian Society of Electron Microscopy, Tampere Finland (2002) 120-121.

[118] E. Césari, V.A. Chernenko, V.V. Kokorin, J. Pons and C. Seguí *Internal friction associated with the structural phase transformations in Ni-Mn-Ga alloys*. Acta Materialia **45** (1997) 999-1004.

[119] C. Seguí, E. Césari, J. Pons and V. Chernenko *Internal friction behaviour of Ni-Mn-Ga.* Materials Science and Engineering A **370** (2003) 481-484.

PUBLICATIONS

I Reprinted from Journal of Applied Physics Vol. **95** *N. Lanska, O. Söderberg, A. Sozinov, Y. Ge, K. Ullakko, V.K. Lindroos,* **Composition and temperature dependence of the crystal structure in Ni-Mn-Ga alloys**, pp. 8074-8078. Copyright (2004), with permission of American Institute of Physics.

II Reprinted from Zeitschrift für Metallkunde Vol. **95** *O. Söderberg, M. Friman, A. Sozinov, N. Lanska, Y. Ge, M. Hämäläinen and V.K. Lindroos***, Transformation behaviour of two Ni-Mn-Ga alloys**, pp. 724-731. Copyright (2004), with permission from Carl Hanser Verlag.

III Reprinted from Journal de Physique IV Vol. **115** *A. Sozinov, A.A. Likhachev, N. Lanska, O. Söderberg, K. Koho, K. Ullakko, V.K. Lindroos,* **Stress-induced variant rearrangement in Ni-Mn-Ga single crystals with nonlayered tetragonal martensitic structure**, pp. 121-128. Copyright (2004), with permission of EDP Sciences.

IV Reprinted from Materials Science and Engineering A Vol. **378/1-2** *A. Sozinov, A.A. Likhachev, N. Lanska, O. Söderberg, K. Ullakko, V.K. Lindroos,* **Stress- and magnetic-field-induced variant rearrangement in Ni-Mn-Ga single crystals with seven-layered martensitic structure**, pp. 399-402. Copyright (2004), with permission from Elsevier.

V Reprinted from Scripta Materialia Vol. **49** *V.G. Gavriljuk, O. Söderberg, V.V. Bliznuk, N.I. Glavatska and V.K. Lindroos,* **Martensitic Transformations and Mobility of Twin Boundaries in Ni_2MnGa Alloys Studied by Using Internal Friction**, pp. 803-809. Copyright (2003), with permission from Elsevier.

VI Reprinted from Materials Science and Engineering A Vol. **386** *O. Söderberg, L. Straka, V. Novák, O. Heczko, S.-P. Hannula and V.K. Lindroos,* **Tensile/compression behavior of non-layered tetragonal $Ni_{52.8}Mn_{25.7}Ga_{21.5}$ alloy**, pp. 27-33. Copyright (2004), with permission from Elsevier.

VII Reprinted from Proceedings of SPIE International Society for Optical Engineering Vol. **5053** *A. Sozinov, A.A. Likhachev, N. Lanska, O. Söderberg, K. Ullakko and V.K. Lindroos***, Effect of crystal structure on magnetic-field-induced strain in Ni-Mn-Ga**, pp. 586-594. Copyright (2003), with permission from SPIE International Society for Optical Engineering.

VIII Reprinted from The Encyclopedia of Materials: Science and Technology Vol. **1** *O. Söderberg, A. Sozinov and V.K. Lindroos* **Giant magnetostrictive materials.** In: J. Buschow (Ed.), pp. 1-3. Copyright (2004), with permission from Elsevier. *In press.*

Studies of the internal friction in Ni-Mn-Ga alloys

Internal friction (IF), the free decay of enforced vibrations, is extremely sensitive to any softening of the crystal lattice. The stress-dependent IF can be used to estimate the value of the activation enthalpy for the movement of the twin boundaries in Ni_2MnGa alloys [*a*]. By measuring the temperature dependence of IF it is possible to detect the possible occurrence of restructuring in martensite. Seguí *et al.* have applied temperature-dependent IF with Ni-Mn-Ga alloys to study the austenite-to-premartensitic transition above M_s [*b*], the double-step martensite transformation [*c*] and the behaviour of three different Ni-Mn-Ga alloys [*d*].

The basic information of the internal friction is given in [*e*]. According to [*b*] the IF curves of the low temperature region have a higher IF level in the martensitic phase than in the parent phase. The two-phase martensite transformation region is shown by an IF peak which is concurrent with the elastic modulus minimum [*b,d*]. According to [*b,d,f*] the IF peak is a result of three factors:

(i) *The intrinsic damping (IF_{int})* of the co-existing phases. This factor is stress amplitude dependent. When the stress is oscillated, IF_{int} is related to the mobility of the defects, including the mobile intervariant boundaries. According to [*a*] in the studied Ni-Mn-Ga alloys this vibration of the twin boundaries is the only mechanism of IF, in the temperature regions where no phase transformations occur.

(ii) *The transient IF (IF_{tr})* related to the transformation kinetics, the non-equilibrium nucleation and growth processes. It depends on the temperature rate involved and it is proportional to the volume fraction transformed per unit time. IF_{tr} is the most important factor at low frequencies (~1 Hz). It is strongly dependent on stress amplitude, temperature rate and frequency. IF_{tr} can be obtained from an isothermal or high frequency IF spectra [*g*].

(iii) *The denominated non-transient or phase transition contribution (IF_s)* appearing during the transformation. It does not depend on the temperature rate. However, it is related to the amount of the transformed volume fraction per stress unit.

(iv) The IF peaks of the martensitic and reverse transformations are connected with the elastic modulus (E) minima of the transformation regions [*b*]. Every point of the amplitude dependent curve $Q^{-1}=f(\varepsilon)$ is proportional to the area or volume involved in oscillation of twin boundaries in respect to their equilibrium position. When the mobility of the twin boundaries increases, larger area/volume is involved to the movement and the elastic energy dissipation is bigger. As a result slope $Q^{-1}(T)=f(\varepsilon)$ is increased. According to [*c*] the high $IF_{tr,mart}$ is assumed to be related to the easy movement of the martensitic intervariant boundaries in the modulated structures. As the mobility of the intervariant boundaries becomes more restricted with decreasing temperature [*g*], the IF should decrease and the E-modulus increase upon cooling. This decrease of the twin variant mobility can be observed as smaller slopes of the IF-strain-curves measured at lower temperatures, since then the vibrations of the twin variants remain nearly unchanged as the strain increases [*a*].

REFERENCES:

[a] V.G. Gavriljuk, O. Söderberg, V.V. Bliznuk, N.I. Glavatska and V.K. Lindroos *Martensitic transformations and mobility of twin boundaries in Ni_2MnGa alloys studied by using internal friction*. Scripta Materialia **49** (2003) 803-809.

[b] E. Césari, V.A. Chernenko, V.V. Kokorin, J. Pons and C. Seguí *Internal friction associated with the structural phase transformations in Ni-Mn-Ga alloys*. Acta Materialia **45** (1997) 999-1004.

[c] C. Seguí, V.A. Chernenko, J. Pons and E. Césari *Two-step martensitic transformation in Ni-Mn-Ga alloys*. Journal de Physique IV **112** (2003) 903-906.

[d] C. Seguí, E. Césari, J. Pons and V. Chernenko *Internal friction behaviour of Ni-Mn-Ga* Materials Science and Engineering A **370** (2003) 481-484.

[e] A.S. Novick and B.S. Berry *Anelastic relaxation in crystalline solids*. New York - London: Academic Press; 1972.

[f] J.E. Bidaux, R. Schaller and W. Benoit, *Study of the H.C.P.-F.C.C. phase transition in cobalt by acoustic measurements,* Acta Metallurgica **37** (1989) 803-811.

[g] R.B. Pérez-Saéz, V. Recarte, M.L. Nó, J. San Juan, *Anelastic contributions and transformed volume fraction during thermoelastic martensitic transformations,* Physical Review B **57** (1998) 5684-5692.

The inverted pendulum equipment applied in the present study

The internal friction measurements were carried out with the automated inverted pendulum equipment at Institute for Metal Physics in Kiev. This equipment is laboratory built. The schematic drawing of the IF equipment and some photos of the construction are shown below in Figures A1-A4.

The pressure in the vacuum chamber is approximately 4 Pa. The accessible temperature range is 77 K – 623 K, but in the applied measurements the maximum measuring temperature was 473 K. The applied linear heating/cooling rate in the measurements was about 1.5 K/min. The strain dependence of the IF at constant temperatures was measured with strain amplitudes 10^{-6}-10^{-4}, where the upper limit was chosen to avoid any strain induced lattice effect. The frequency range depends on the sample size and the elastic constants of the studied alloy. During the measurements of the present work the frequency range was 0.5-3 Hz, while the sample length was fixed to 65 mm and the cross section of the samples varied in between (3-5) x 2 mm^2.

M1-M4
permanent magnets
L1-L4
exiting and measuring coils of electromagnets

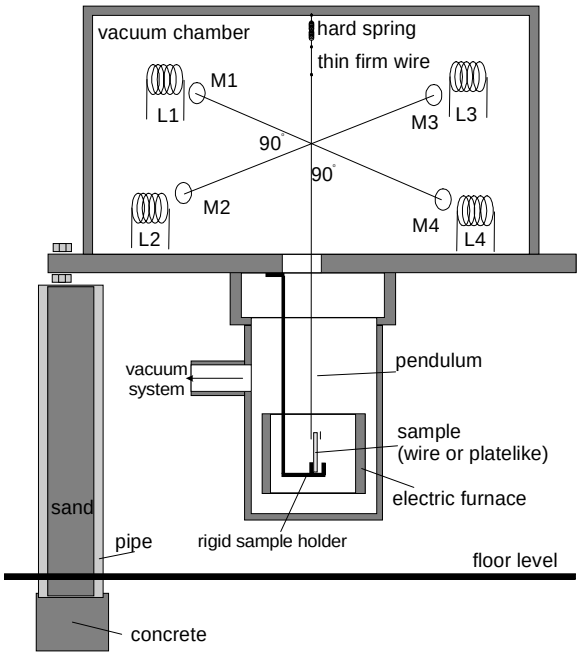

Figure A1.
Schematic drawing of the inverted pendulum equipment for the measurements of the internal friction (IF-equipment).

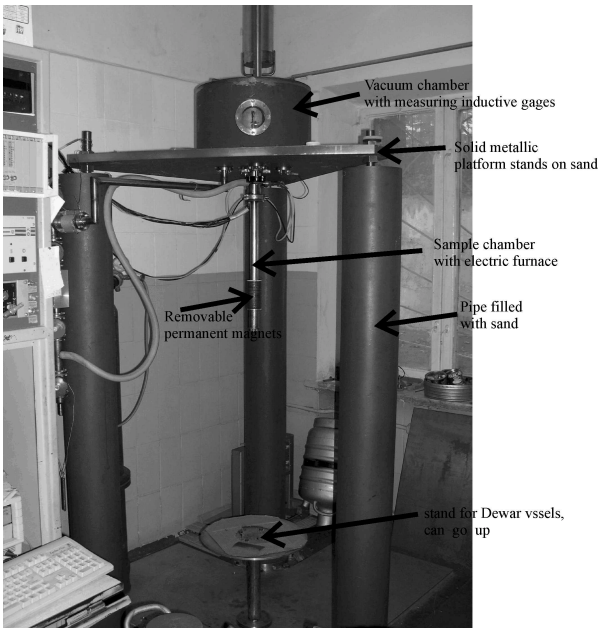

Figure A2.
The set-up of the IF-equipment.

Figure A3.
The turbo molecular vacuum pump attached to the IF-equipment.

Figure A4.
The set-up of the control unit of the IF-equipment.